Calhoun
Institutional Archive of the Naval Postgraduate School

Calhoun: The NPS Institutional Archive

Theses and Dissertations Thesis Collection

1984-09

Experimental investigation of turbulent heat transfer in straight and curved rectangular ducts

Daughety. Steven Floyd

http://hdl.handle.net/10945/19330

DUDLEY KNOX LIBRARY

Calhoun is a project of the Dudley Knox Library at NPS, furthering the precepts and goals of open government and government transparency. All information contained herein has been approved for release by the NPS Public Affairs Officer.

Dudley Knox Library / Naval Postgraduate School
411 Dyer Road / 1 University Circle
Monterey, California USA 93943

http://www.nps.edu/library

DUDLEY KNOX LIBRARY
NAVAL POSTGRADUATE SCHOOL
MONTEREY, CALIFORNIA 93943

NAVAL POSTGRADUATE SCHOOL
Monterey, California

THESIS

EXPERIMENTAL INVESTIGATION OF TURBULENT HEAT TRANSFER IN STRAIGHT AND CURVED RECTANGULAR DUCTS

by

Joel L. Wilson

December 1984

Thesis Advisor: M. D. Kelleher

Approved for public release; distribution unlimited.

T223280

REPORT DOCUMENTATION PAGE	READ INSTRUCTIONS BEFORE COMPLETING FORM
1. REPORT NUMBER / 2. GOVT ACCESSION NO.	3. RECIPIENT'S CATALOG NUMBER
4. TITLE (and Subtitle) Experimental Investigation of Turbulent Heat Transfer in Straight and Curved Rectangular Ducts	5. TYPE OF REPORT & PERIOD COVERED Master's Thesis December 1984 6. PERFORMING ORG. REPORT NUMBER
7. AUTHOR(s) Joel L. Wilson	8. CONTRACT OR GRANT NUMBER(s)
9. PERFORMING ORGANIZATION NAME AND ADDRESS Naval Postgraduate School Monterey, California 93943	10. PROGRAM ELEMENT, PROJECT, TASK AREA & WORK UNIT NUMBERS
11. CONTROLLING OFFICE NAME AND ADDRESS Naval Postgraduate School Monterey, California 93943	12. REPORT DATE December 1984 13. NUMBER OF PAGES 81
14. MONITORING AGENCY NAME & ADDRESS (if different from Controlling Office)	15. SECURITY CLASS. (of this report) Unclassified 15a. DECLASSIFICATION/DOWNGRADING SCHEDULE

16. DISTRIBUTION STATEMENT (of this Report)

Approved for public release; distribution unlimited.

17. DISTRIBUTION STATEMENT (of the abstract entered in Block 20, if different from Report)

18. SUPPLEMENTARY NOTES

19. KEY WORDS (Continue on reverse side if necessary and identify by block number)

Taylor-Gortler Vortices, heat transfer, secondary flow, rectangular curved channel, rectangular straight channel, Temsheet, Joulean heating, turbulent flow.

20. ABSTRACT (Continue on reverse side if necessary and identify by block number)

An experimental investigation has been conducted to examine the convective heat transfer in straight and curved ducts of rectangular cross section. The experimental configuration was modeled as infinite parallel plates with one wall at a constant heat flux and the opposite wall adiabatic. Experiments were conducted at steady state for turbulent flow using average Nusselt numbers to compare the heat transfer characteristics of the straight and curved sections.

The development of Taylor-Gortler vortices in the curved section proved to enhance the heat transfer rate over that of the straight section. Improved heat exchanger and turbine blade design could both result from a better understanding of the effects of curvature on the rate of heat transfer.

Approved for public release; distribution unlimited.

Experimental Investigation of Turbulent Heat Transfer in Straight and Curved Rectangular Ducts

by

Joel L. Wilson
Lieutenant, United States Navy
B.S., United States Naval Academy, 1977

Submitted in partial fulfillment of the
requirements for the degree of

MASTER OF SCIENCE IN MECHANICAL ENGINEERING

from the

NAVAL POSTGRADUATE SCHOOL
December 1984

John N. Dyer, Dean of Science and Engineering

ABSTRACT

An experimental investigation has been conducted to examine the convective heat transfer in straight and curved ducts of rectangular cross section. The experimental configuration was modeled as infinite parallel plates with one wall at a constant heat flux and the opposite wall adiabatic. Experiments were conducted [illegible] steady state for turbulent flow using average Nusselt numbers to compare the heat transfer characteristics of the straight and curved sections.

The development of Taylor-Gortler vortices in the curved section proved to enhance the heat transfer rate over that of the straight section. Improved heat exchanger and turbine blade design could both result from a better understanding of the effects of curvature on the rate of heat transfer.

TABLE OF CONTENTS

I. INTRODUCTION -- 14

A. TAYLOR-GORTLER VORTICES ---------------------- 14

B. HISTORY -- 16

II. INTENT OF THE STUDY ------------------------------ 22

III. EXPERIMENTAL WORK -------------------------------- 24

A. DESCRIPTION OF THE APPARATUS ----------------- 24

B. EXPERIMENTAL PROCEDURES ---------------------- 37

IV. PRESENTATION OF DATA ----------------------------- 41

A. ANALYSIS --------------------------------------- 41

B. RESULTS -- 43

V. DISCUSSION AND CONCLUSIONS ----------------------- 56

VI. RECOMMENDATIONS ---------------------------------- 65

APPENDIX A: EXPERIMENTAL UNCERTAINTY ------------------ 66

APPENDIX B: SAMPLE CALCULATIONS ---------------------- 69

A. SAMPLE CALCULATION DATA ----------------------- 70

B. TEMPERATURE CALCULATIONS --------------------- 71

C. POWER CALCULATIONS --------------------------- 71

D. MASS FLOW RATE CALCULATIONS ------------------ 72

E. REYNOLDS NUMBER CALCULATIONS ----------------- 74

F. HEAT CONVECTED TO AIR CALCULATION ------------ 74

G. AVERAGE HEAT TRANSFER COEFFICIENT CALCULATION- 75

H. AVERAGE NUSSELT NUMBER CALCULATION------------ 75

I. DEAN NUMBER CALCULATION----------------------- 75

APPENDIX C: CORRELATIONS ------------------------------ 76

LIST OF REFERENCES ------------------------------------ 78

INITIAL DISTRIBUTION LIST ------------------------------ 81

LIST OF TABLES

I. Summary of Straight Test Section Results (Large Orifice) -- 44

II. Summary of Straight Test Section Results (Small Orifice - Untripped) ------------------------- 45

III. Summary of Straight Test Section Results (Small Orifice - Tripped) --------------------------- 46

IV. Summary of Curved Test Section Results (Large Orifice) -- 47

V. Summary of Curved Test Section Results (Small Orifice) -- 48

LIST OF FIGURES

1. Schematic of Taylor-Gortler Vortices in a Curved Channel.---------------------------------- 15

2. Schematic of Taylor Vortices between Cylinders.----- 18

3. Illustration of Equipment and Apparatus.------------ 25

4. Cross-sectional View of Channel.-------------------- 26

5. Straight Test Section, Detailed Schematic.---------- 29

6. Curved Test Section, Detailed Schematic.------------ 30

7. Thermocouple Placement in Test Sections.------------ 33

8. Photograph of Test Channel.------------------------- 34

9. Photograph of Flow Measuring Apparatus.------------- 35

10. Photograph of Data Acquisition System.-------------- 36

11. Circuit Used to Measure Power Supplied to the Temsheet.------------------------------------ 40

12. Straight vs. Curved Section Results Present Study.--------------------------------------- 49

13. Liquid Crystal Representation of Airflow. (Curved Section, Re_{hd} = 1100) ---------------------- 53

14. Liquid Crystal Representation of Airflow. (Curved Section, Re_{hd} = 9400) ---------------------- 53

15. Liquid Crystal Representation of Airflow. (Straight Section, Re_{hd} = 12700) ------------------ 54

16. Liquid Crystal Representation of Airflow. (Straight Section, Re_{hd} = 4000, Untripped) --------- 55

17. Liquid Crystal Representation of Airflow. (Straight Section, Re_{hd} = 4000, Tripped) ----------- 55

18. Comparison of Straight Section Present Data with Daughety, Holihan, and Ballard.---------------- 58

19. Comparison of Curved Section Present Data with Daughety, Holihan, and Ballard.---------------------- 59

20. Comparison of Both Sections Present Data with Daughety, Holihan, and Ballard.---------------------- 60

21. Comparison of Straight Section Present Data with Dittus-Boelter, Petukhov and Popov, Kays and Leung, an Extrapolated Kays and Leung, and a Calculated Least Squares Fit.---------------------- 62

22. Comparison of Curved Section Present Data with Petukhov and Popov, Brinich and Graham, a Calculated Least Squares Fit, and an Extrapolated Least Squares Fit.---------------------- 63

23. Energy Balance in Straight Section.------------------ 69

TABLE OF SYMBOLS

Symbol	Meaning	Units
A	cross-sectional area of the orifice	m^2
A_c	cross-sectional area of the channel	m^2
A_{pipe}	cross-sectional area of the pipe	m^2
A_{PL}	area of the wall heater (Temsheet)	m^2
C_{pair}	specific heat of air at constant pressure	J/KgK
Dc	channel height	m
De	Dean number	
D_{hd}	hydraulic diameter	m
D_{orif}	diameter of the orifice	m
D_{pipe}	diameter of the pipe	m
F_{wo-wi}	radiation shape factor	
g_c		$\frac{Kg\ m}{N\ sec^2}$
$\overline{h}$	average heat transfer coefficient	W/m^2C
K	flow coefficient	
K_{air}	thermal conductivity of air	W/mC
K_{ins}	thermal conductivity of insulation	W/mC
$\dot{m}$	mass flow rate of air	Kg/sec
Nu	local Nusselt number	
$\overline{Nu}$	average Nusselt number	
Pr	Prandtl number	
P_{atm}	atmospheric pressure	N/m^2

Symbol	Meaning	Units
P_1	pressure upstream of orifice	N/m^2
P_{wet}	wetted perimeter of channel	m
Q_{air}	heat convected to the air	W
Q_{li}	heat lost through inner wall (Plexiglas)	W
Q_{lo}	heat lost through outer wall (Temsheet)	W
Q_n	power supplied	W
Q_r	heat transferred by radiation	W
R	gas constant for air	Nm/Kg K
Re_d	Reynolds number based on channel height	
Re_{hd}	Reynolds number based on hydraulic diameter	
Re_{nine}	Reynolds number based on pipe diameter	
Ri	radius of curvature of inner convex wall	m
R_{PR}	electrical resistance of precision resistor	Ω
R_R	total radiation resistance	m^{-2}
Ta	Taylor number	
T_{blk}	bulk temperature of flow	C
T_{in}	average flow inlet temperature	C
T_{ins1}	temperature between first and second layers of insulation	C
T_{ins2}	temperature between second and third layers of insulation	C
T_{orif}	temperature of air flowing downstream of orifice	C
T_{out}	average flow outlet temperature	C

Symbol	Meaning	Units
T_{wi}	average temperature of inner wall	C
T_{wo}	average temperature of outer wall	C
V_{PR}	voltage across precision resistor	V
V_H	voltage across the wall heater (Temsheet)	V
Y	expansion factor	
β	ratio of orifice diameter to pipe diameter	
ε_{wi}	emissivity of inner wall (Plexiglas)	
ε_{wo}	emissivity of outer wall (Temsheet)	
γ	ratio of specific heats of air	
μ_{air}	dynamic viscosity of air	Kg/m sec
ρ_{air}	density of air	Kg/m^3
σ	Stefan-Boltzmann constant	W/m^2K^4
ΔP	pressure drop across the orifice	N/m^2
ΔT	mean temperature difference	C
ΔT_{ins}	temperature difference in insulation	C
ΔX_{ins}	thickness of insulation layers	m

ACKNOWLEDGEMENT

The author wishes to express his sincere appreciation to Professor Matthew D. Kelleher for his valuable advice and assistance throughout the term of this project, without which this thesis would have proven a nearly insurmountable task.

The shop personnel also deserve a special thanks for their assistance and skill in the construction of the experimental apparatus.

I. INTRODUCTION

A. TAYLOR-GORTLER VORTICES

Since the early part of the twentieth century, considerable research has shown that fully developed laminar flow along a concave wall does not remain two-dimensional [Refs. 1, 2, 3]. The flow instead forms a system of spiral vortices, of counter rotating pairs, whose axes are aligned in the principle flow direction. This phenomenon is the result of the variations in the centrifugal forces acting on the fluid particles, and is known as Taylor-Gortler vortices. Figure 1 illustrates the type of fluid motion just described.

In a channel that is curved in the streamwise direction, those fluid particles located in the center of the flow cross-section are subjected to higher centrifugal forces than those fluid particles traveling along the channel's boundary wall. As a result, the fluid in the center of the channel moves outwardly towards the concave boundary. As the process continues, the fluid particles near the boundary wall, move in a spanwise direction, and finally radially inward replacing the outwardly moving particles. These particles then come under the same centrifugal forces and the process repeats itself. The resulting cyclic motion causes the formation of the counter-rotating Taylor-Gortler vortices, considered to be primarily a laminar flow phenomenon.

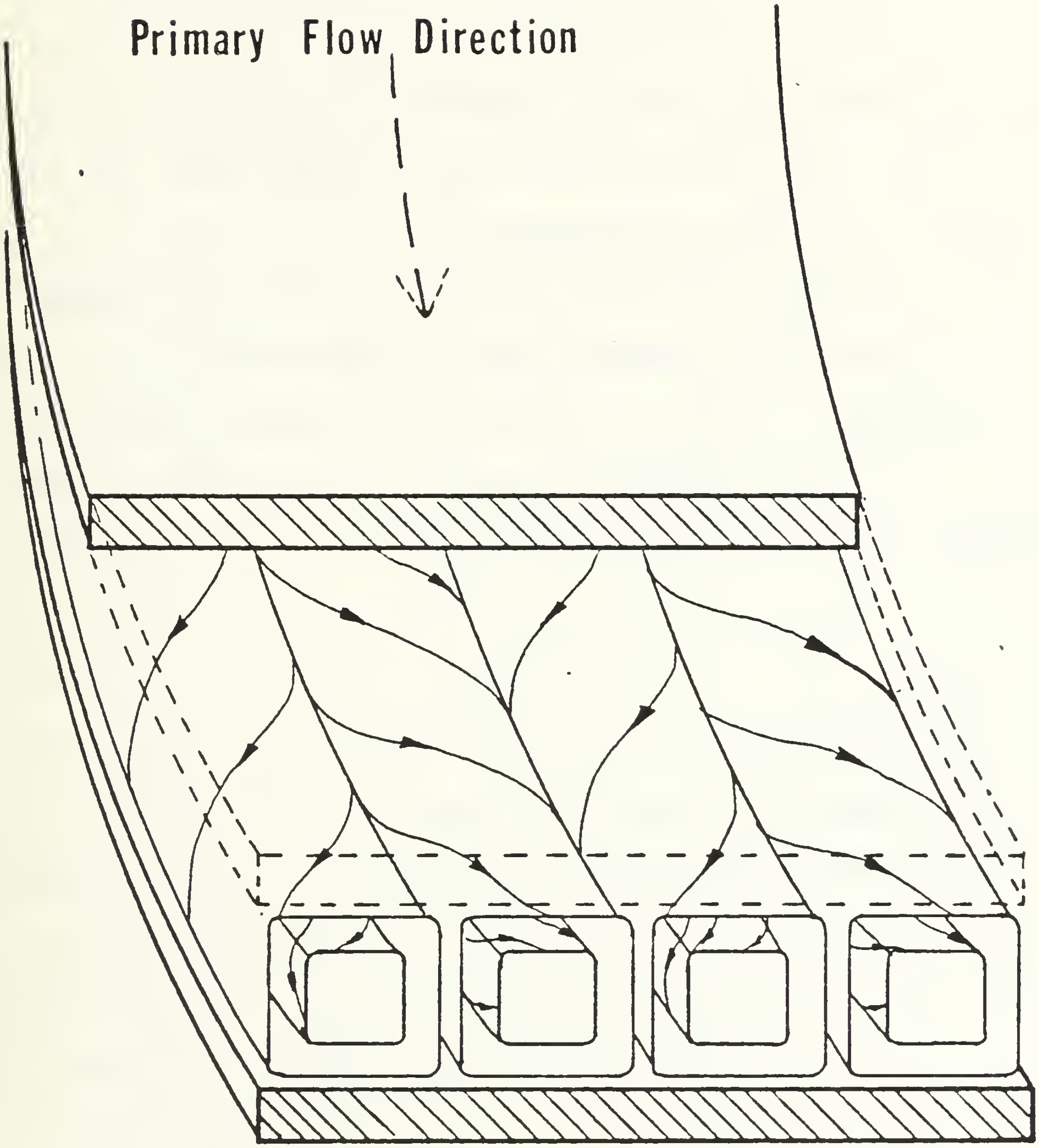
Primary Flow Direction

Figure 1. Schematic of Taylor-Gortler Vortices in a Curved Channel.

It has been observed [Ref. 4] that the heat transfer rate from flow along a concave curved wall is greater than that for flow along a straight wall, a phenomenon attributed to the additional mixing provided by the secondary motion of the Taylor-Gortler vortices. It is thought that the crosshatching observed on reentry vehicles can be explained in part by the presence of streamwise vortices similar to the Taylor-Gortler vortice phenomenon.

There are many possible applications that could result from a more thorough understanding of Taylor-Gortler vortices and their effect on heat transfer and fluid flow characteristics. Two such applications could lead to improved heat exchanger designs and improved turbine blade cooling [Refs. 5, 6, 7].

B. HISTORY

The instability of an inviscid fluid flowing past a curved boundary, was first considered by Lord Rayleigh in 1916 [Ref. 8]. By assuming that the fluid was non-viscous, he determined that for the motion of an inviscid fluid to remain stable, its circulation must increase with increasing radius. G. I. Taylor, in 1923, [Refs. 1, 9], continued this study with an extensive analytical and experimental study of viscous fluids. His investigations focused on the flow between two cylinders, in which the inner cylinder rotated while the outer cylinder remained stationary. Taylor ascertained that such flows become unstable when the value of a dimensionless parameter exceeded a critical value of 41.3. The parameter, known as the Taylor number is defined as:

$$Ta = Re \sqrt{\frac{d}{Ri}}$$

where 'd' is the width of the gap, assumed small when compared to 'Ri', the radius of the inner cylinder, and 'Re' is the Reynolds number based on the peripheral velocity of the inner cylinder. Taylor determined that for those cases in which the value of the Taylor number exceeded the critical value, a secondary motion developed and the Taylor vortices formed. Figure 2 illustrates this fluid motion.

Instability of a similar nature is also observed when a viscous fluid flows in a curved channel due to a pressure gradient acting along the channel wall. This problem was first considered analytically by W. R. Dean [Ref. 10] in 1928, for a channel formed by two concentric cylinders, where the radius of the inner cylinder was large in comparison to the spacing between the inner and outer cylinder walls. Dean concluded that there would be an initiation of flow instability, and the formation of vortices, when a dimensionless parameter, the Dean number, exceeded a value of 36. The Dean number is defined as:

$$De = Re \sqrt{\frac{d}{Ri}}$$

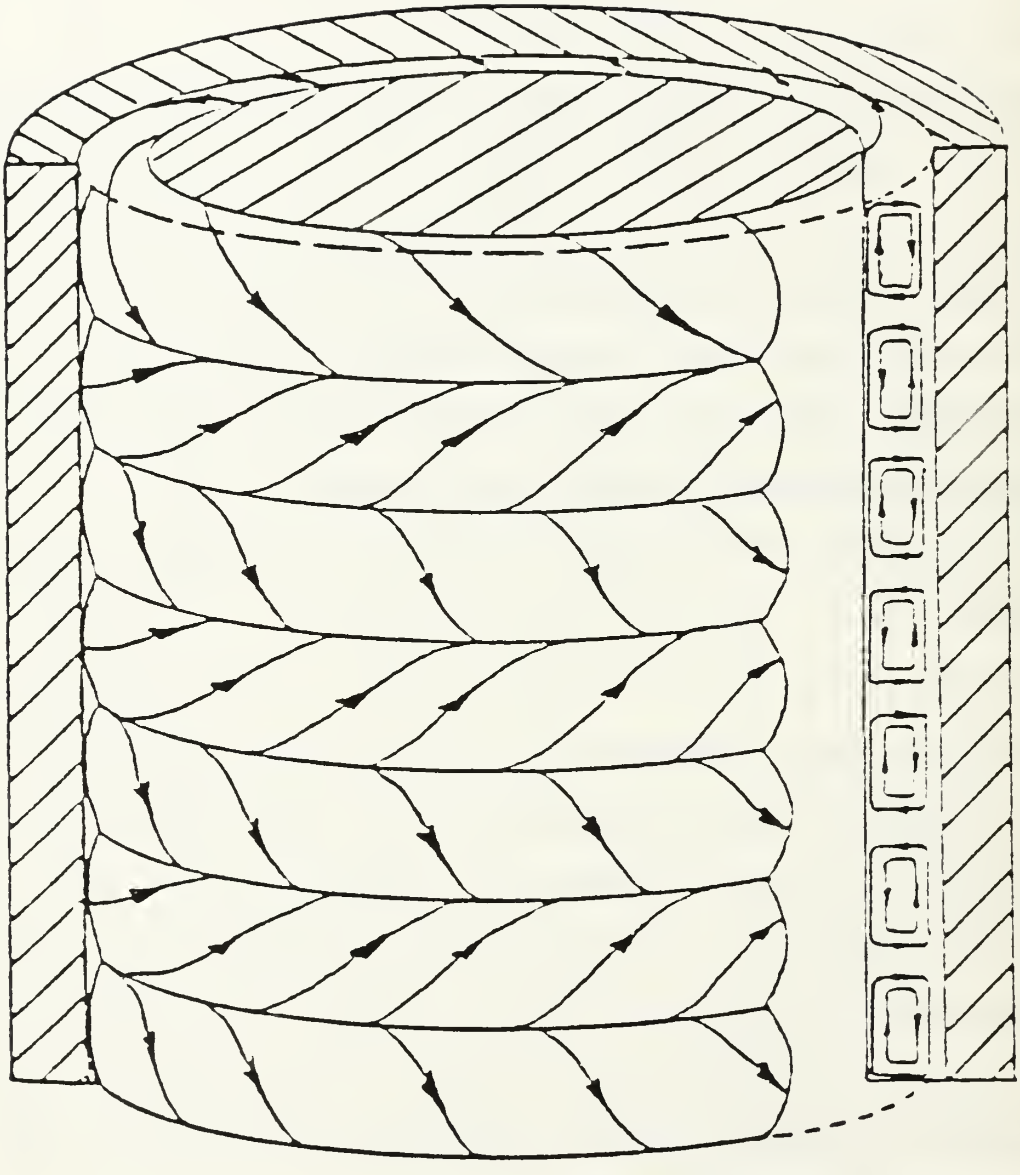

Figure 2. Schematic of Taylor Vortices between Cylinders.

REPRODUCED AT GOVERNMENT EXPENSE

where 'd' represents the channel half-width, 'Ri' is the inner cylinder radius, and 'Re' is the Reynolds number based on the mean velocity of the undisturbed flow and the channel half width 'd'. The analytical work of Dean was later verified by W. H. Reid [Ref. 11], using an approximate solution.

In 1940, H. Gortler [Ref. 2] studied the stability of laminar boundary layer profiles on curved walls under the influence of small disturbances. He found that these disturbances were similar to the vortices studied by G. I. Taylor. Using approximate numerical calculations, Gortler concluded that the disturbances or vortices were produced only on the concave boundary walls and that the overall flow profile appeared to remain laminar in nature. These results were verified, with an exact solution, by G. Hammerlin, and reported by H. Schlichting [Ref. 12] in 1955. A. M. O. Smith completed an even more extensive numerical analysis that further substantiated these findings [Ref. 3]. The results of these numerical solutions have recently been demonstrated with the use of hot wire anemometry, laser doppler systems, and flow visualization techniques, [Refs. 13, 14]; and in 1976, Y. Aihara [Ref. 15] conducted a non-linear analysis of Gortler vortices.

As interest began to develop concerning the effects of the secondary flows associated with the Taylor-Gortler vortices, many studies were published concerning the influences of these vortices on heat transfer in the laminar and turbulent flow regimes. In 1955, F. Kreith [Ref. 16], studied the influence of heat transfer with respect to the curvature of the boundary wall for fully turbulent flows. He concluded that the heat transfer from the heated concave boundary wall was considerably higher than that transferred from the convex boundary wall of the same curvature and under similar turbulent conditions.

In 1965, L. Persen [Ref. 17], considered the special cases of very high and very low Prandtl number fluids and related the increase in heat transfer from a curved wall to the presence of the Taylor-Gortler vortices.

There has been only a limited amount of published literature dealing with the flow and heat transfer in curved channels of rectangular cross-section and large aspect ratios, where the aspect ratio is equal to the spanwise distance of the channel divided by the channel height. Much of what has been published involves the development of numerical approximations and solutions for heat and mass transfer in curved ducts of various geometries. K. Cheng and M. Akiyama [Ref. 18] developed a numerical solution for forced convection heat transfer with laminar flows in curved channels of rectangular cross-section, but only for small aspect ratios.

In 1976, A. A. Shibani and M. N. Ozisik [Ref. 19], using matched asymptotic expansion techniques for a wide range of Prandtl numbers, solved the heat transfer problem between parallel plates with turbulent flow, for the case of uniform wall temperature.

Other experimental and analytical studies that are worth citing with regard to this present study follow. Y. Mori [Ref. 20], obtained results for hydrodynamically fully developed flows with constant wall heat flux, in curved channels of square cross-section. W. M. Kays and E. Y. Leung [Ref. 21] reported solutions for turbulent flow heat transfer in a concentric circular tube annulus with a fully developed velocity profile and constant heat rate per unit length, for a fluid of Prandtl number 0.7. Results for large aspect ratio channels with rectangular cross-sections for laminar flows were reported by M. Durao [Ref. 22] and J. Ballard [Ref. 23]. R. Holihan, Jr. [Ref. 24] reported results for laminar and transition flows and S. F. Daughety [Ref. 25] reported results for turbulent flows. P. F. Brinich and R. W. Graham [Ref. 26] reported results for turbulent flows in a rectangular curved channel with an aspect ratio of 6, for the inner wall heated, the outer wall heated, and both walls heated.

II. INTENT OF THE STUDY

The purpose of this investigation was to examine the effect of streamwise curvature on the heat transfer rate in a curved rectangular duct of large aspect ratio, again defining aspect ratio as the spanwise distance divided by the channel height. The flow velocities examined were in the transition and turbulent regime. The results of this study were compared to the heat transfer rates for the same range of velocities, in a straight duct of identical aspect ratio.

Although Taylor-Gortler vortices are considered to be a laminar flow phenomenon, enhanced heat transfer in curved channels for transition and turbulent flows has been observed. Even though it has not been proven that the vortices continue to propagate at the higher flow velocities, this enhancement in the transfer of heat has been attributed to the secondary flow velocity components of the Taylor-Gortler vortices. It is believed that these secondary components transport the heated fluid from the outer concave wall, inward toward the opposite wall of the channel, displacing the cooler fluid particles and causing them to move toward the heated concave wall. It was expected that similar results would be observed in this study.

This investigation was conducted using a single channel with a rectangular cross-section and constant aspect ratio. The channel incorporated both a straight test section and a curved test section. The results obtained in each test section at approximately the same flow rates were compared in an effort to determine the effects of the Taylor-Gortler vortices on the transfer of heat. Also, the results of both the straight and curved sections were compared to the results of Ballard [Ref. 23], Holihan [Ref. 24], and Daughety [Ref. 25].

The straight section results of this study were compared to the Dittus-Boelter equation for flows in circular tubes [Ref. 26], the results of Kays and Leung for turbulent and transition flow in annular passages [Ref. 21], and the analytical solutions of Petukhov and Popov for transition flows in circular tubes [Ref. 27].

The curved section results of this study were compared with the results of Brinich and Graham [Ref. 28] for turbulent flow in a rectangular curved channel, and also to the solutions of Petukhov and Popov, mentioned above.

III. EXPERIMENTAL WORK

A. DESCRIPTION OF THE APPARATUS

To meet the objectives of this investigation, a channel of rectangular cross-section was used. Details of its construction are described in references 22 and 23. Plexiglas, 0.635 centimeters thick, formed the inner and outer walls of the channel. These walls were separated by 0.635 centimeter spacers that also served as the sides of the channel.

The channel, shown in Figure 3, had a straight section, 122.0 centimeters in length, followed by a curved section of 180 degrees of arc, followed by another straight section, 91.4 centimeters in length. The inner curved wall of the channel had a radius of curvature of 30.5 centimeters. The rectangular channel was 0.635 centimeters high and 25.4 centimeters wide resulting in an aspect ratio of 40. The hydraulic diameter was 1.229 centimeters. The cross-sectional area of the channel was 16.13 square centimeters. The wetted perimeter was 52.07 centimeters. Figure 4 shows a cross-sectional view representing both the straight and curved sections of the channel.

An entrance bell constructed of plexiglas was connected to the straight section of the channel. It was designed and manufactured according to ASME nozzle standards, with an elliptical curved base on a major axis equal to ten inches

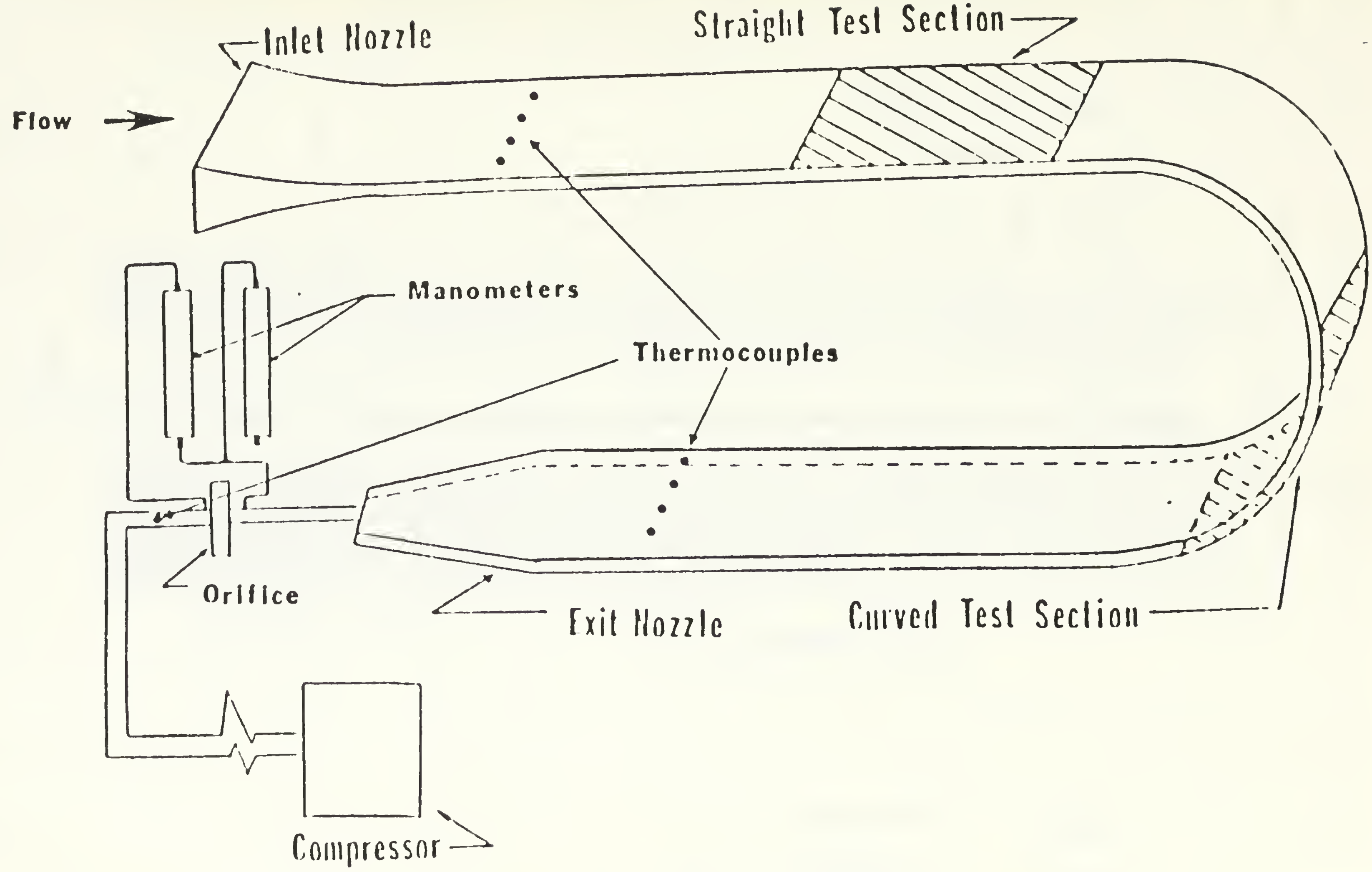
Inlet Nozzle
Straight Test Section
Flow
Manometers
Thermocouples
Orifice
Exit Nozzle
Curved Test Section
Compressor

Figure 3. Illustration of Equipment and Apparatus.

REPRODUCED AT GOVERNMENT EXPENSE

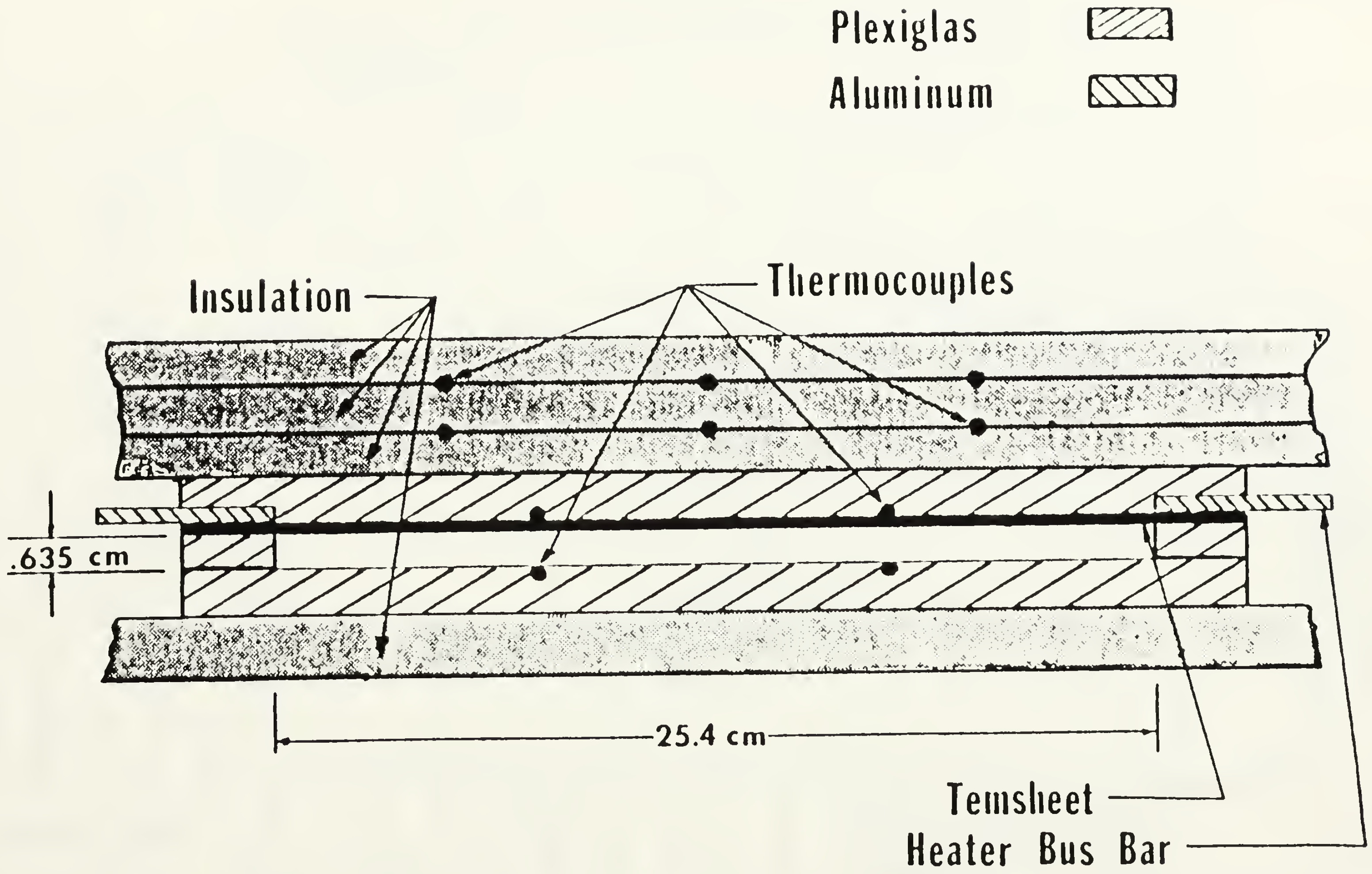
Plexiglas ▨
Aluminum ▧
Insulation
Thermocouples
.635 cm
25.4 cm
Temsheet
Heater Bus Bar

Figure 4. Cross-sectional View of Channel.

and a minor axis of one inch. Cheese-cloth was attached to the entrance nozzle to prevent foreign matter from entering the flow channel. An aluminum exhaust nozzle was attached to the exit of the channel and directed the flow from the channel into two inch diameter pvc piping. The two inch pvc piping contained a measuring section which could be fitted with standard ASME concentric orifices. In this study two orifice plates were used. An orifice with a diameter of 0.5325 inches was used for hydraulic Reynold's numbers below 5000, and an orifice with a diameter of 1.065 inches was used for hydraulic Reynold's numbers above 5000. Pressure taps on either side of the orifice, at 1 and 1/2 pipe diameters, and connected to manometers were used to calculate the mass flow rate of the working fluid, which was air at room temperature.

The flow of air was drawn through the channel by an electrically driven Spencer Turbo Compressor, rated 30 horsepower at 3500 rpm, and 550 cubic feet per minute at 70 degrees fahrenheit and one atmosphere.

The channel contained two test sections from which experimental heat transfer data could be obtained. The straight test section was located 120 centimeters downstream of the entrance bell to ensure hydrodynamically fully developed flow. The straight test section was 29.2 centimeters in length with a heated test section area of 741.7 square centimeters. The curved test section was located in the lower half of the curved portion of the channel. It was 28.3 centimeters in length, subtending an arc of 53.1 degrees, and having a heated test section area of 718.4 square centimeters.

In each of the heated test sections, Temsheet, a carbon impregnated porous paper with a uniform electrical resistivity, was glued to the outer wall. Joulean heating was used to heat the flow of air through the channel. Since the electrical resistance of the Temsheet is not constant, but varies slowly with temperature, a precision resistor with an electrical resistance of 2.0262 ohms was connected in series with the Temsheet to allow the calculation of the instantaneous power being supplied. Detailed schematics of each test section are shown in Figures 5 and 6.

The variables that were measured and used in this investigation were:

(1) the temperature of the air entering the channel (T_{in})
(2) the temperature of the air leaving the channel (T_{out})
(3) the temperature of the heated outer wall for each test section (T_{wo})
(4) the temperature of the unheated inner wall for each test section (T_{wi})
(5) the temperature between the three layers of insulation at each test section (T_{ins})
(6) the voltage across the precision resistor (V_r)
(7) the voltage across the Temsheet or heater (V_h)

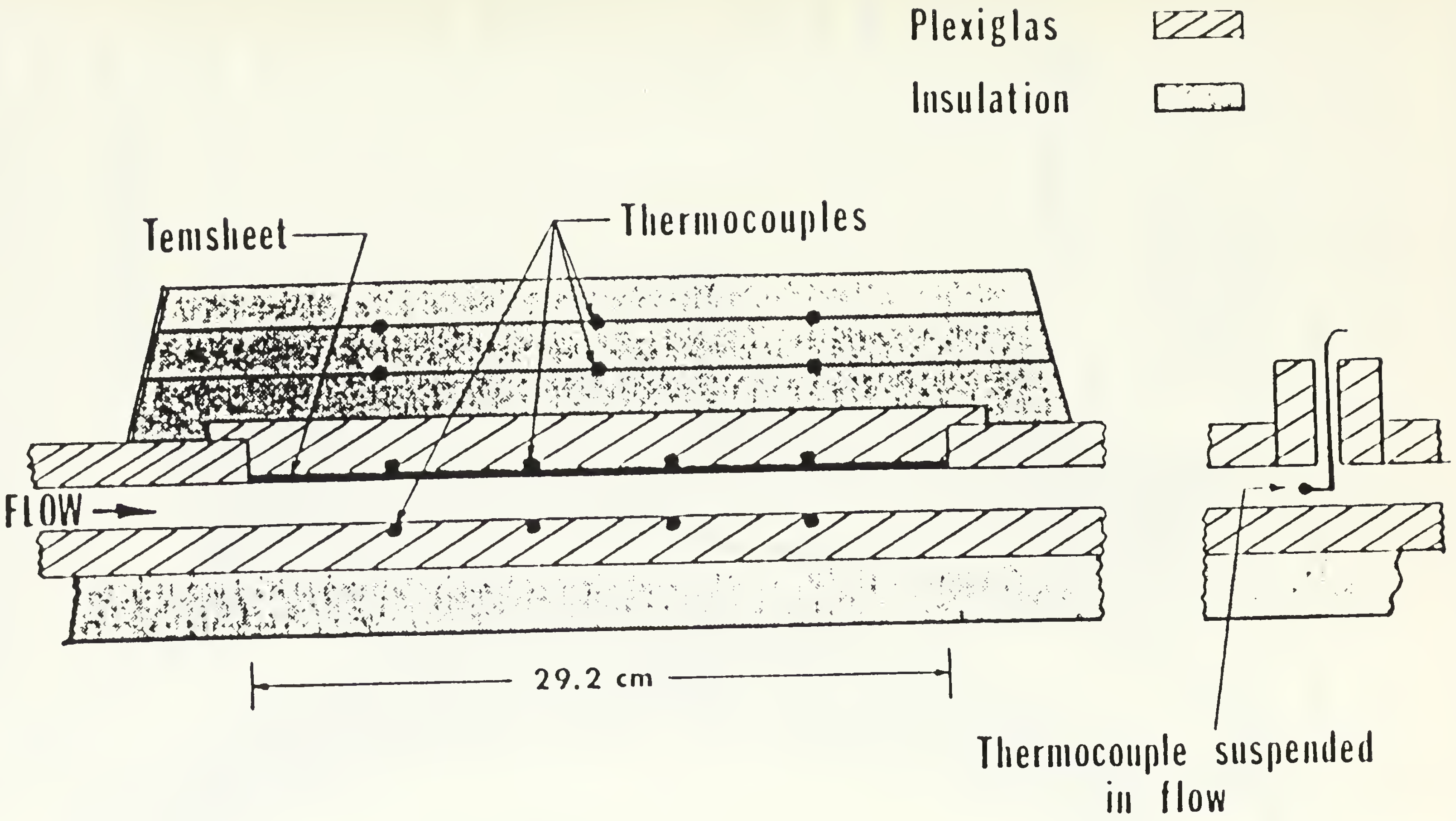
Plexiglas ▨
Insulation ☐
Temsheet
Thermocouples
FLOW
29.2 cm
Thermocouple suspended in flow

Figure 5. Straight Test Section, Detailed Schematic.

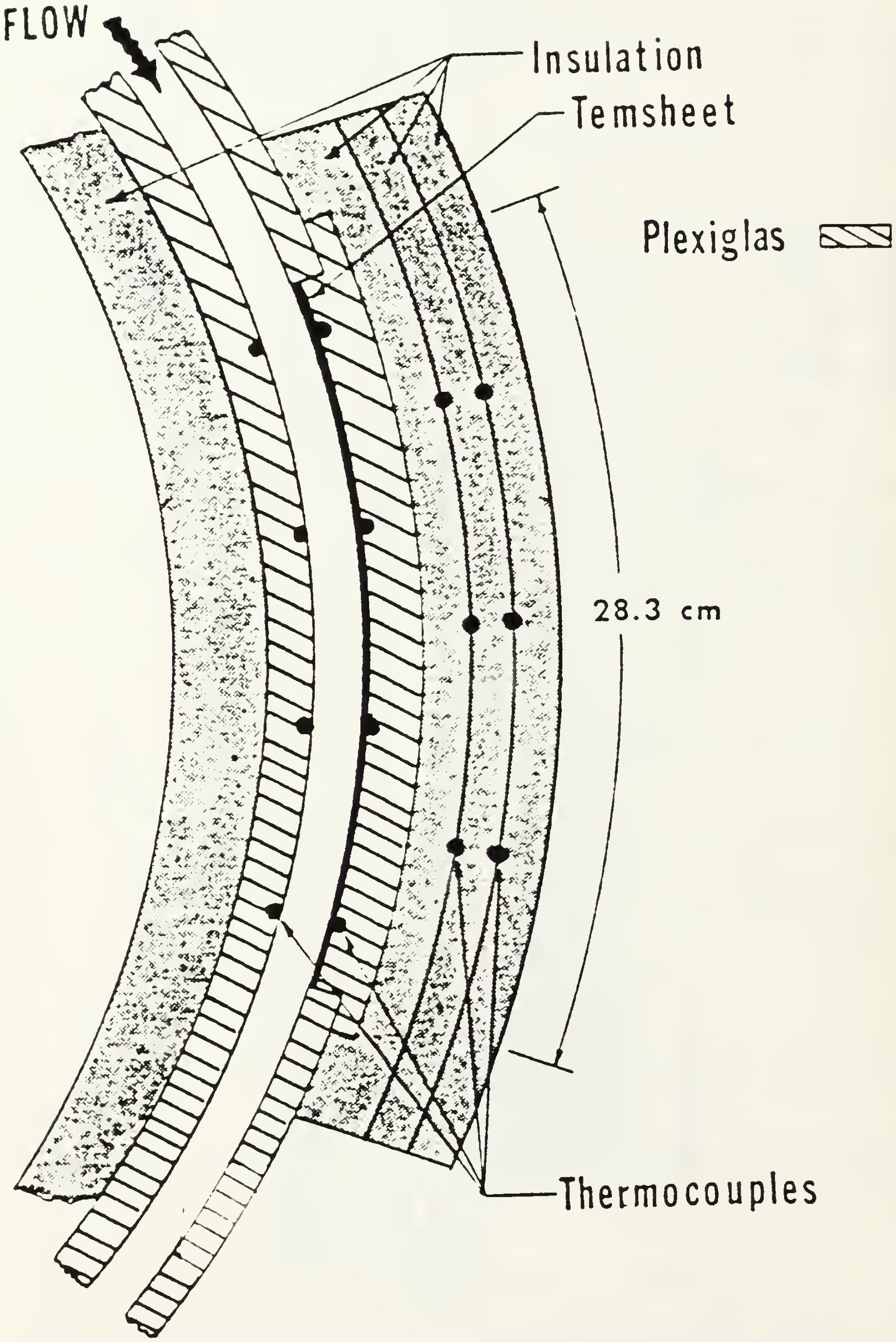
FLOW
Insulation
Temsheet
Plexiglas ▨
28.3 cm
Thermocouples

Figure 6. Curved Test Section, Detailed Schematic.

(8) the temperature of the air at the orifice (T_{orif})

(9) the pressure upstream of the orifice (P_{up})

(10) the difference in the upstream and the downstream pressure across the orifice (ΔP)

(11) the atmospheric pressure (P_{atm})

A total of sixty-one Copper-Constantan, 30 gauge thermocouples were located throughout the test apparatus to record the desired temperatures. Readings from four thermocouples spanning the width of the channel were averaged to give the temperature at the entrance and exit to the channel. Five thermocouples were connected in parallel and inserted between each of the layers of insulation at each of the test sections. In addition, individual thermocouples were positioned in each of the test sections, eight in direct contact with the Temsheet and eight in the plexiglas of the unheated inner wall. The beads of the thermocouples in contact with the Temsheet were electrically insulated with ENMAR Heat Resisting Glyceryl Phthalate. Small diameter holes were drilled in the plexiglas to allow the installation of the thermocouples. One thermocouple was inserted in the two inch pvc pipe downstream of the orifice in accordance with the ASME Power Test Code to record the temperature of the air flowing through the orifice.

The thermal insulation consisted of 1/2 inch layers of Armstrong Armaflex 22 Sheet Insulation, a flexible foamed plastic material. By positioning thermocouples between these insulation layers, the heat lost to the environment could be computed at each test section. The heat loss through insulation surrounding the rest of the channel due to the heated air flowing through the channel was small in comparison. See Figure 7 for a detailed sketch of the thermocouple placement and attachment. The insulation was held in place by the use of velcro strips attached to the frame. The entire channel and all connections between the channel, the pvc piping, and the orifice were sealed with General Electrical Silicone Rubber Sealant Caulk to ensure there was no leakage of air into the channel or the piping which could affect the recorded temperatures or mass flow rate.

The data acquisition system used for this experiment was a Hewlett Packard 3054A Automatic Data Acquisition/Control System consisting of a 3456A Digital Voltmeter and a 3497A Data Acquisition/Control Unit. Also used in conjunction with this data acquisition system, were a Hewlett Packard 9326 Computer terminal and 2671G Printer. Pressure measurements were taken from Meriam vertical manometers, one whose fluid was water with a 0 to 60 inch range, another using water with a 0 to 30 inch range, and a third whose fluid was mercury, calibrated to read inches of water with a range of 0 to 415 inches. A photograph of the channel and associated test equipment are shown in Figures 8, 9, and 10.

REPRODUCED AT GOVERNMENT EXPENSE

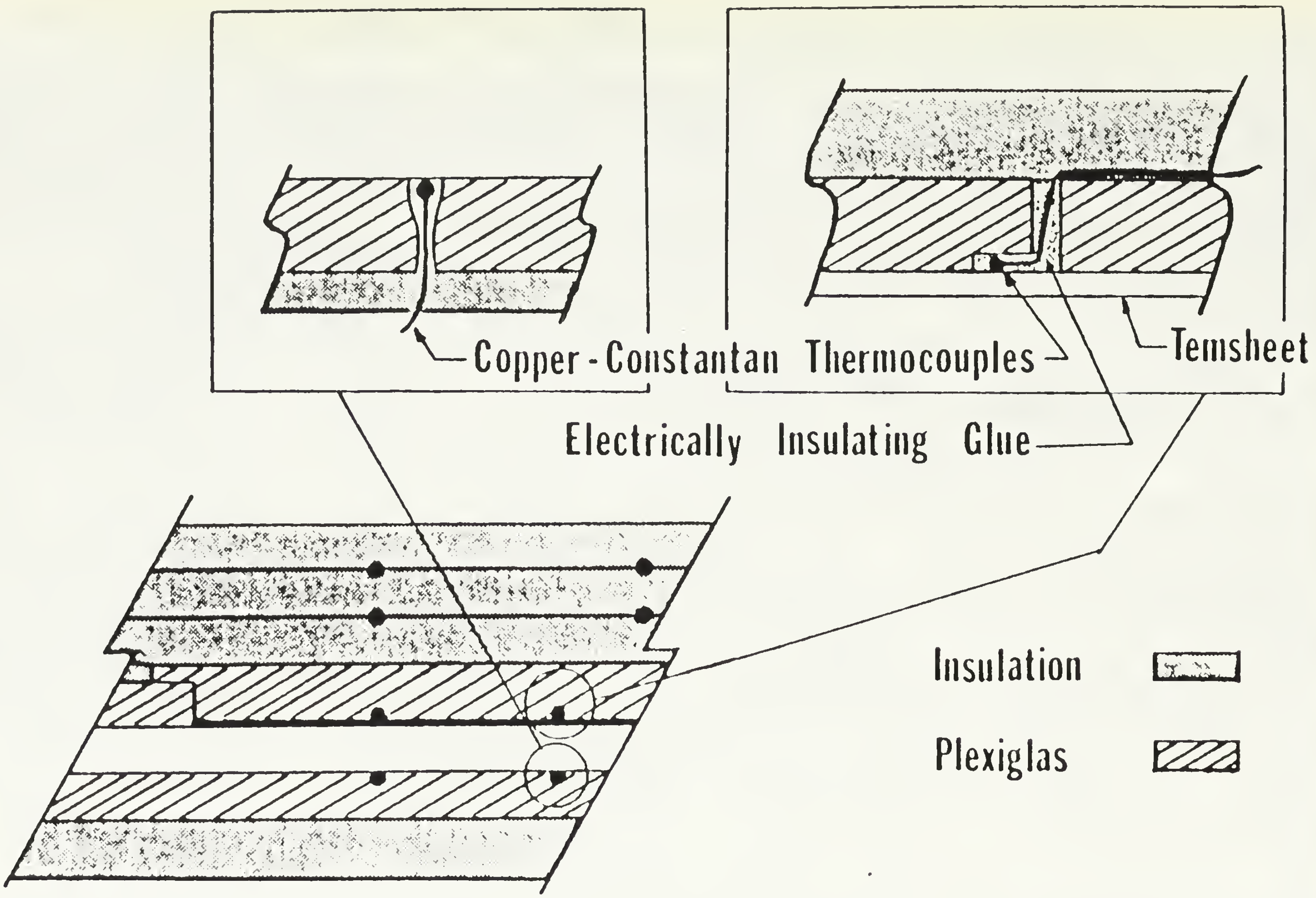
Copper-Constantan Thermocouples
Temsheet
Electrically Insulating Glue
Insulation ▨
Plexiglas ▨

Figure 7. Thermocouple Placement in Test Sections.

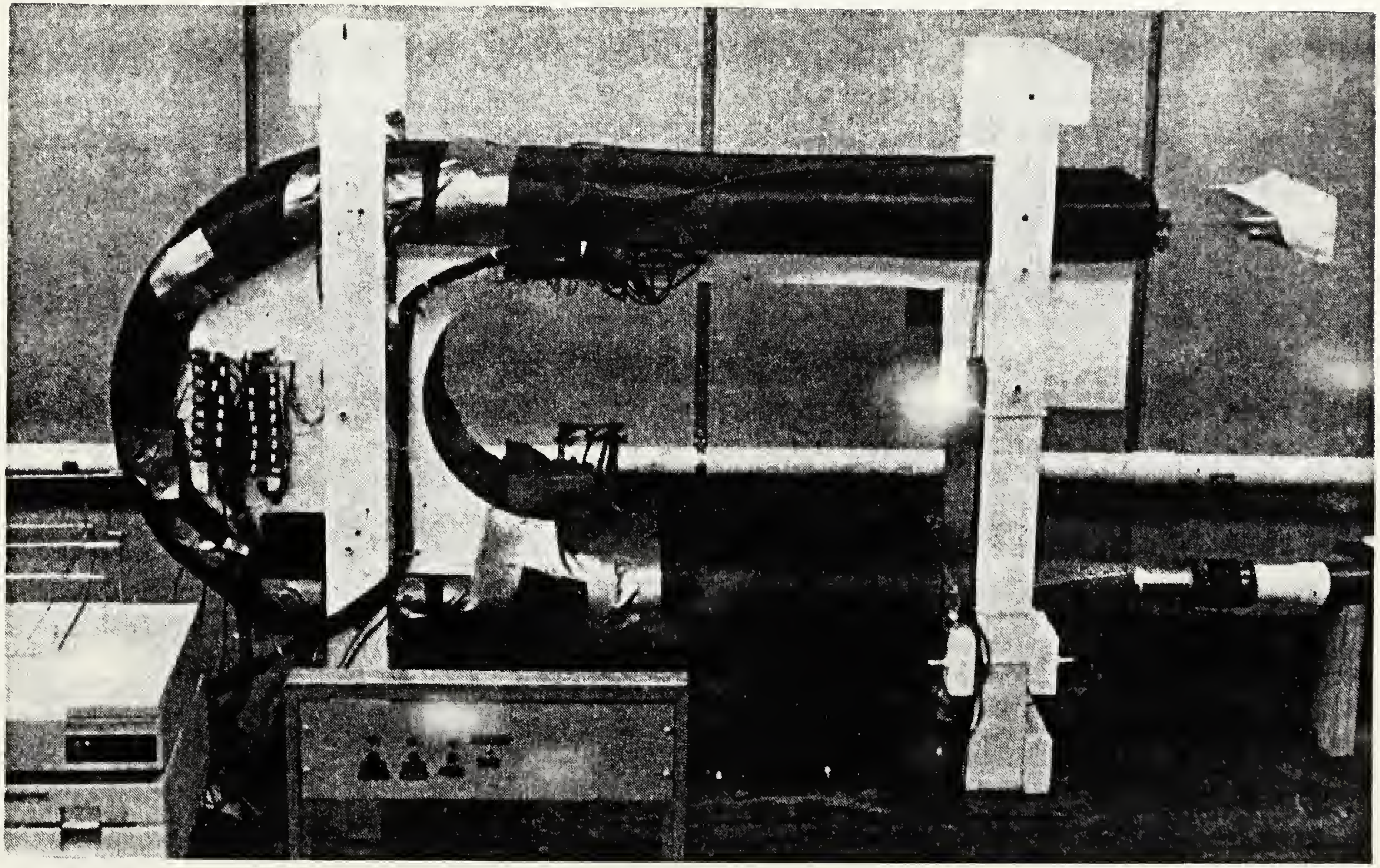

Figure 8. Photograph of Test Channel.

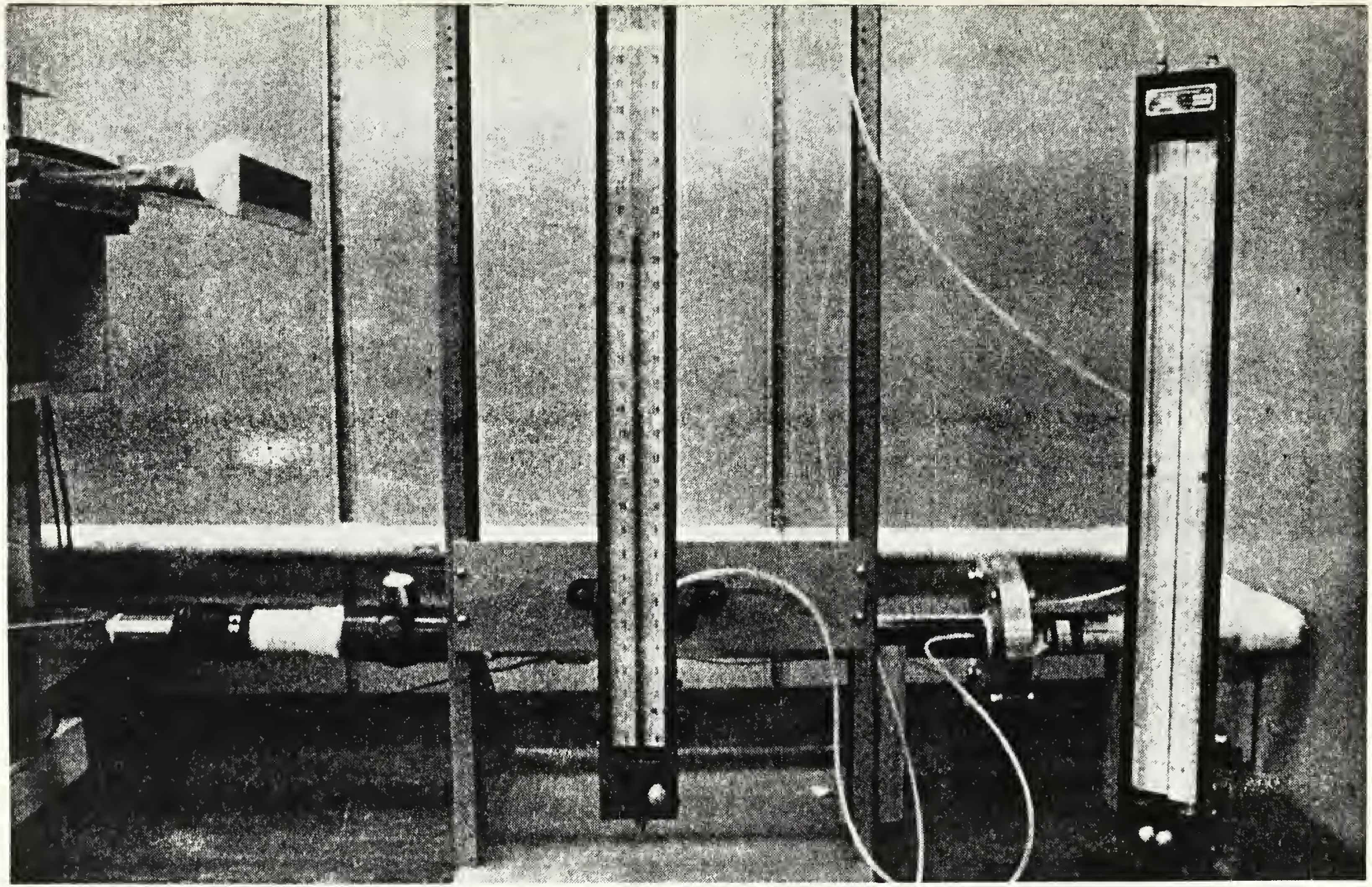

Figure 9. Photograph of Flow Measuring Apparatus.

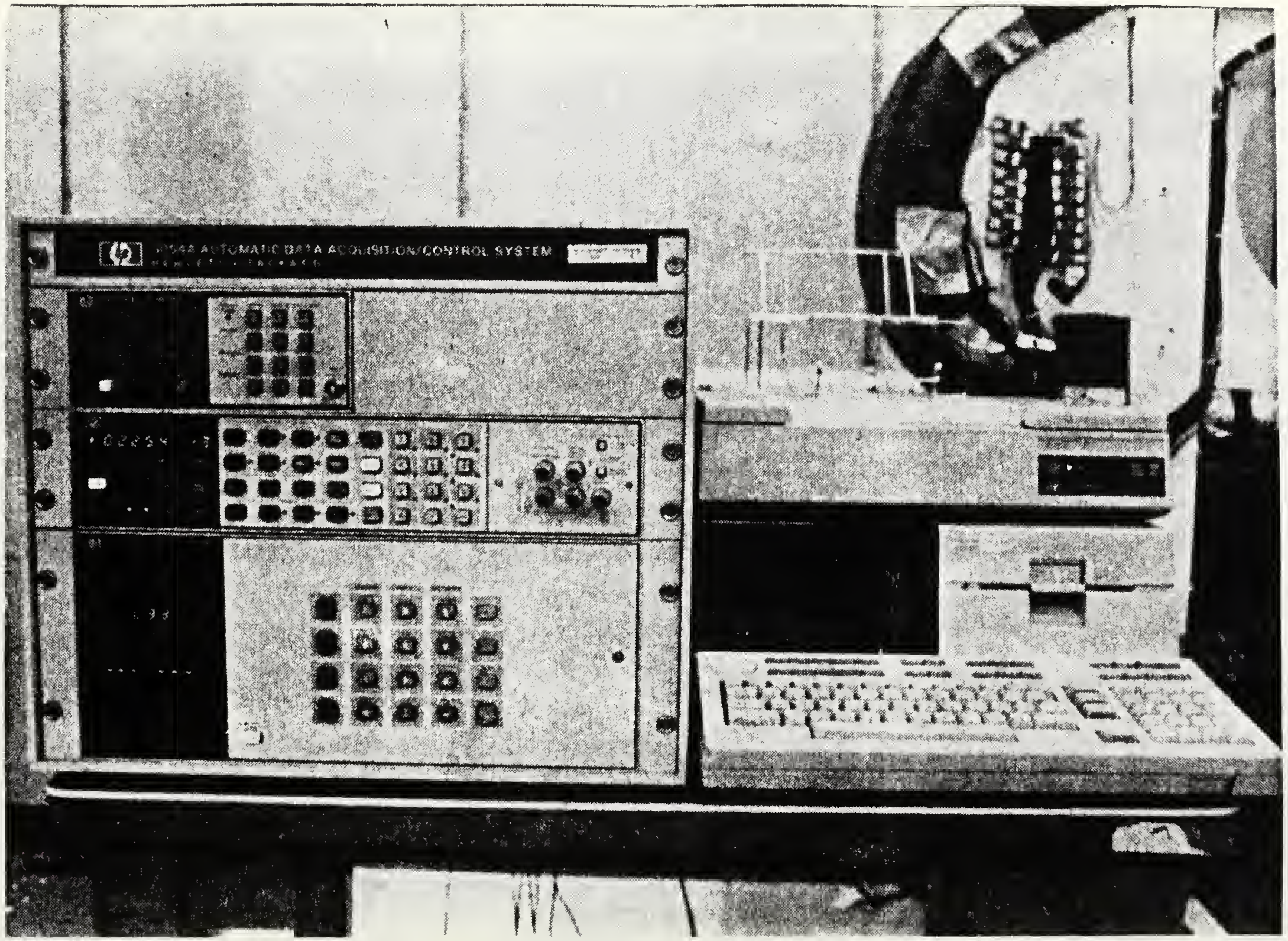
AUTOMATIC DATA ACQUISITION/CONTROL SYSTEM

Figure 10.' Photograph of Data Acquisition System.

Sheets of cholesteric liquid crystal slurries with a temperature range of 40-43^{O}C were used to provide qualitative measurements of the surface temperature distribution on the Temsheet. The liquid crystals exhibit dramatic color changes over a small temperature differential and allow a reasonable comparison to be made between the heat transfer processes on each test section by observation of the color pattern displayed for varying temperature gradients and flow velocities. Specifically, the occurrence of multi-colored stripes aligned in the flow direction on the curved wall would indicate regions of high and low temperatures and confirm the presence of Taylor-Gortler vortices.

The addition of this liquid crystal sheet necessitated a calculation of its overall heat transfer coefficient. To determine the true surface temperature of the heated wall the temperature drop across the sheet must be known. The sheet was composed of 4.5 mils of a liquid crystal slurry with approximately the same thermal conductivity as body fat, .5 mils of acrylic backing, and a 2 mil mylar cover; resulting in an overall heat transfer coefficient of 522 w/^{O}C. Insulation opposite the heated sections was fitted with removable panels to allow viewing and photographing of the liquid crystals.

B. EXPERIMENTAL PROCEDURES

The experimental procedures followed were the same for the straight and curved test sections. The results obtained from the straight test section served as a baseline for the comparison of the curved section results. Experiments were conducted by varying the mass flow rate of air corresponding to Reynolds numbers from approximately 800 to 25000, where the Reynolds numbers are based on hydraulic diameter. For each mass flow rate, data was taken automatically by the data acquisition system and the data was immediately reduced and printed. Preliminary runs were performed to determine the time required for the test rig to come to steady state. For this experiment three hours were allowed for steady state to be reached. After three hours, data was taken at ten minute intervals to ensure that a steady state condition had been achieved. The criteria for steady state was based on three variables:

(1) the difference between inlet and outlet temperature

(2) the heated boundary wall temperature

(3) the unaccounted heat loss in the system

When the first two of these variables varied by less than two percent over a ten minute interval and the third began to fluctuate, it was considered that a steady state condition had been achieved.

It was also necessary to determine the approximate power setting required to bring the heated wall of each test section to approximately 50 degrees Centigrade. It had been determined by Holihan [Ref. 24] that this temperature was sufficient to ensure a 20 degree Centigrade difference in the heated wall and the unheated wall.

For each run, the atmospheric pressure, the pressure difference across the orifice, and the pressure upstream of the orifice were entered into the computer for the mass flow rate calculations. All other data was acquired by the data acquisition system directly from the experimental apparatus.

To compute the instantaneous power supplied the following relationship was used:

$$Q_p = \frac{V_H \, V_R}{R_{PR}}$$

The precision resistor voltage and the heater voltage were read by the data acquisition system and the resistance of the precision resistor was a known constant. A diagram of this circuit is shown in Figure 11.

Upon completion of selected data runs photographs were taken of the liquid crystals on the heated section to provide a visual record of the airflow patterns.

For Reynolds numbers ranging from approximately 2400 to 5600, it was necessary to make two sets of data runs for the straight test section. The first, with conditions the same as for other flow rates, which exhibited a pronounced deviation from the near linear results; and a second, where the flow just prior to the straight test section was tripped with sandpaper, which reestablished the near linear results. This reproducible anamoly indicated the presence of a transition region between laminar and turbulent flow.

REPRODUCED AT GOVERNMENT EXPENSE

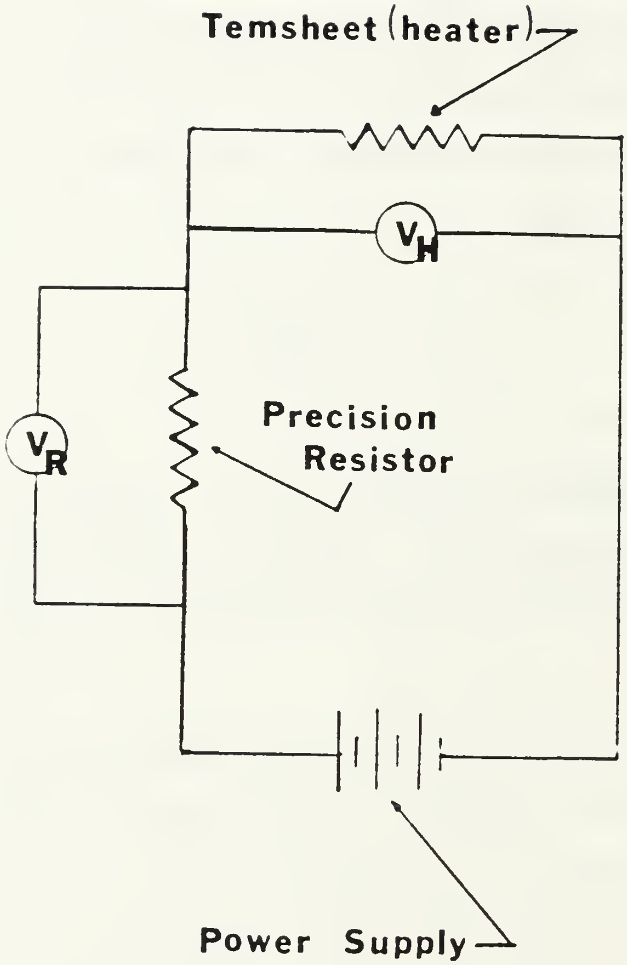
Temsheet (heater)
V_H
V_R
Precision Resistor
Power Supply

Figure 11. Circuit Used to Measure Power Supplied to the Temsheet.

IV. PRESENTATION OF DATA

A. ANALYSIS

The constant heat flux surface for the heated wall of each test section was provided by the uniform electrical resistivity of the Temsheet. The insulated unheated wall was considered adiabatic since the heat losses through that wall were negligible. The channel's large aspect ratio of 40 allowed the modeling of the channel as parallel plates. The straight portion of the channel upstream of the straight test section was of sufficient length to ensure that the flow was hydrodynamically developed for the flow velocities of this study. The straight portion of the channel downstream of the curved test section was also of sufficient length to ensure that the flow exiting the channel was thoroughly mixed and that the temperature, T_{out}, was an average bulk temperature.

Based on these assumptions, the experimental configuration was modeled as forced convection between parallel plates, for hydrodynamically developed and thermally developing flows, subjected to a constant heat flux. The boundary conditions are one wall at a constant heat flux and the other wall insulated.

To analyze this problem, several quantities were defined as follows;

The heat convected to the air was calculated using the equation:

$$Q_{air} = \dot{m}\, C_{pair}(T_{out} - T_{in})$$

where 'C_{pair}' was the specific heat of the air at constant pressure and '$\dot{m}$' was the mass flow rate of the air. Mass flow rate was calculated using standard ASME flow measurement techniques [Ref. 33].

The average heat transfer coefficient between the heated wall and the flow of air in the channel was defined by the equation:

$$\bar{h} = \frac{Q_{air}}{A_{PL}\, \Delta T}$$

where 'Q_{air}' is defined above, 'A_{PL}' was the area of the Temsheet in the test section, and 'ΔT' was the difference between the arithmetic average heated wall temperature (T_{wo}) and the average bulk air temperature (T_{blk}). The average bulk temperature was defined as the arithmetic mean of the entrance and exit temperatures (T_{in}, T_{out}).

The average Nusselt number was then calculated using:

$$\overline{Nu}_{hd} = \frac{\bar{h}\, D_{hd}}{K_{air}}$$

In this equation 'D_{hd}' is the hydraulic diameter and 'K_{air}' is the thermal conductivity of air.

The Reynolds number was calculated for each test run as follows:

$$Re_{hd} = \frac{\dot{m}\, D_{hd}}{A_c\, \mu_{air}}$$

where again '$\dot{m}$' and 'D_{hd}' are the mass flow rate and hydraulic diameter of the channel, 'A_c' is the cross-sectional area of the channel, and 'μ_{air}' is the dynamic viscosity of the air.

For the curved section runs the Dean number was defined as:

$$De = Re_{hd} \sqrt{\frac{D_{hd}}{Ri}}$$

where 'Re_{hd}' is the Reynolds number based on the hydraulic diameter, 'D_{hd}' is the hydraulic diameter, and 'Ri' is the radius of curvature of the unheated inner convex wall.

A sketch of the control volume and a set of sample calculations for one test run of the curved section are given in Appendix B. A sample calculation for the uncertainty analysis is given in Appendix A.

B. RESULTS

The data obtained from each experimental run was evaluated utilizing the expressions described in Part A above. The major parameters resulting from this evaluation are shown in Tables I through V. Tables I through III contain the straight section results and Tables IV and V contain the results of the curved section. A plot of the average Nusselt number verses Reynolds number is given in Figure 12 for the comparison of the results. Figure 12 shows the flow passing through the transition regime of the straight section in both the

Table I

Summary of Straight Test Section Results (Large Orifice)

Re_{hd}	Q_{air} (W)	$\bar{h}$ (W/mC)	ΔT (C)	$\overline{Nu}_{hd}$
4973	47.09	30.80	20.61	14.97
5633	67.70	35.65	25.60	17.26
6326	83.83	39.19	28.83	18.81
7096	75.40	44.41	22.88	21.54
7989	98.82	47.99	27.75	23.09
8935	82.48	52.05	21.36	25.10
9969	101.85	56.20	24.43	27.29
11520	121.29	63.12	25.90	30.52
12772	120.00	67.01	24.13	32.35
14357	122.20	73.52	22.40	35.43
16137	122.09	77.78	21.16	37.50
17990	124.29	83.17	20.14	40.55
20629	125.30	89.53	18.86	43.82
24507	127.56	101.13	17.00	48.63

Reynolds number and Nusslet number are based on hydraulic diameter.

Table II

Summary of Straight Test Section Results (Small Orifice - Untripped)

Re_{hd}	Q_{air} (W)	$\bar{h}$ (W/mC)	ΔT (C)	$\overline{Nu}_{hd}$
1524	27.17	14.74	24.84	7.20
2162	32.19	18.92	22.93	9.20
2686	34.81	19.03	24.65	9.23
3321	39.19	21.67	24.37	10.57
4063	40.31	23.27	23.34	11.00
4463	39.28	23.83	22.21	11.60
4851	52.09	26.41	26.58	12.77
5223	51.15	30.97	22.25	15.18

Reynolds number and Nusselt number are based on hydraulic diameter.

Table III

Summary of Straight Test Section Results
(Small Orifice - Tripped)

Re_{hd}	Q_{air} (W)	$\overline{h}$ (W/mC)	ΔT (C)	$\overline{Nu}_{hd}$
1976	41.74	17.91	31.40	8.62
2354	34.35	19.87	23.30	9.62
2793	40.11	22.55	23.97	10.88
3225	35.37	24.52	19.44	11.95
3626	50.87	28.29	24.23	13.72
4639	50.47	33.84	20.10	16.44
5552	51.99	39.33	17.81	19.18
7014	72.53	45.85	21.32	22.27

Reynolds number and Nusselt number are based on draulic diameter.

Table IV

Summary of Curved Test Section Results
(Large Orifice)

Re_{hd}	De	Q_{air} (W)	$\bar{h}$ (W/mC)	ΔT (C)	$\overline{Nu}_{hd}$
4952	2257	79.49	41.71	26.11	20.39
5650	2574	72.36	44.95	22.05	21.97
6560	2989	82.47	50.05	22.57	24.20
7578	3453	81.40	54.48	20.47	26.39
8444	3847	97.95	59.04	22.73	28.56
10000	4555	103.57	64.62	21.96	31.11
10972	4999	105.79	68.81	21.06	33.80
11515	5256	108.32	72.74	20.40	34.97
12067	5498	110.84	72.50	20.94	35.41
13000	5922	114.52	79.05	19.84	38.19
13723	6252	116.24	82.86	19.22	40.34
14493	6602	118.59	86.79	18.72	42.36
17238	7854	121.95	99.76	16.75	48.41
20517	9348	124.65	113.84	15.00	55.50
24208	11029	126.31	126.43	13.68	61.20

Reynolds number and Nusselt number are based on hydraulic diameter.

Table V

Summary of Curved Test Section Results
(Small Orifice)

Re_{hd}	De	Q_{air} (W)	$\bar{h}$ (W/mC)	ΔT (C)	$\overline{Nu}_{hd}$
1550	706	39.59	22.75	23.84	10.86
1828	833	40.55	24.86	22.35	12.04
2150	978	54.24	27.41	27.11	13.10
2426	1105	50.84	29.66	23.48	14.27
2751	1254	48.48	30.38	21.86	14.83
3372	1536	49.48	33.56	20.20	16.00
3815	1738	51.06	36.39	19.22	17.65
4312	1964	71.12	39.11	24.91	19.05
5215	2378	72.52	44.02	22.57	21.22

Reynolds number and Nusselt number are based on hydraulic diameter.

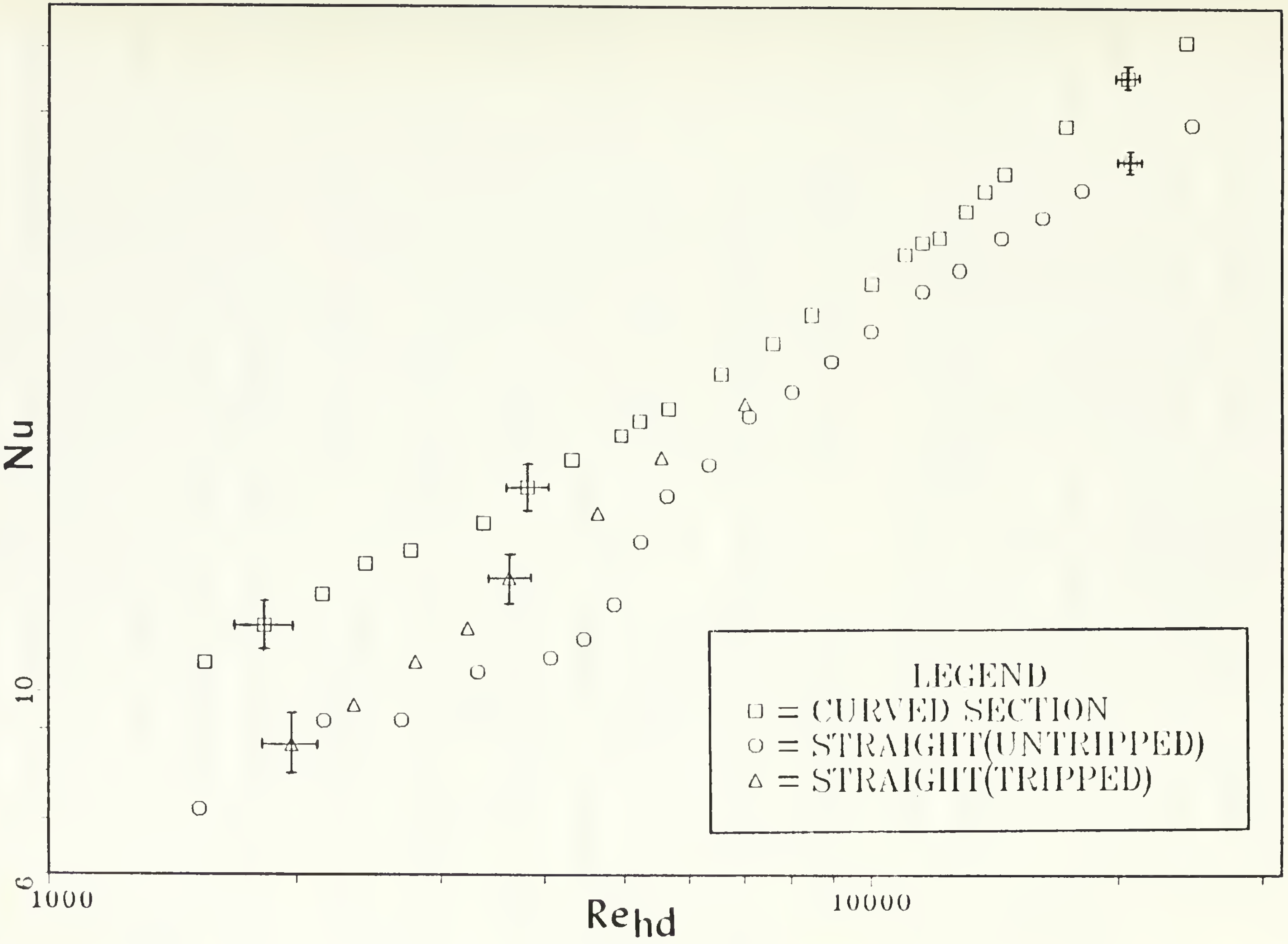

Figure 12. Straight vs. Curved Section Results Present Study.

tripped and untripped condition. All further comparisons will be conducted using the data from the tripped flow.

The results indicate an increase in the rate of heat transfer with increasing Reynolds number for both the straight and curved test sections. In addition, the heat transfer rate was higher in the curved section for each Reynolds number investigated.

A straight line least squares correlation of the data for the present study resulted in:

$$\overline{Nu} = 0.02\ Re_{hd}^{0.79} \qquad 2300 < Re_{hd} < 7100$$

for transition flow in the straight test section;

$$\overline{Nu} = 0.22\ Re_{hd}^{0.53} \qquad 1500 < Re_{hd} < 5300$$

for transition flow in the curved test section;

$$\overline{Nu} = 0.07\ Re_{hd}^{0.65} \qquad 8900 < Re_{hd} < 25000$$

for turbulent flow in the straight test section; and

$$\overline{Nu} = 0.03\ Re_{hd}^{0.76} \qquad 8400 < Re_{hd} < 25000$$

for turbulent flow in the curved test section.

In the short laminar regime of this study the rate of heat transfer was about forty-five percent higher in the curved section, indicating the presence of Taylor-Gortler vortices. As flow progressed through the transition regime a loss of enhancement of heat transfer rate, from forty to about twenty percent, was observed as flow over the straight section went from laminar to fully turbulent. In the low end of the turbulent regime, Reynolds number between 5400 and 12000, the rate of heat transfer was about thirteen percent higher in the curved section. As the Reynolds number continued to increase beyond 12000 so did the enhancement of heat transfer, to approximately twenty-six percent at 24000. This compares favorably with earlier studies by Kreith [Ref. 16], where he reported an increase in the rate of heat transfer along a concave wall of from twenty-five to sixty percent for Reynolds numbers, based on hydraulic diameter, between 10^4 and 10^6. Holihan reported an increase of fifteen percent for laminar flow and thirty percent for transition flow [Ref. 24]. Ballard reported an increase of eleven percent in the heat transfer rate for laminar flows [Ref. 23]. Daughety reported an increase of twenty percent in the heat transfer for turbulent flows [Ref. 25].

The actual presence of Taylor-Gortler vortices was verified by the observation of the liquid crystal isotherm distribution in the curved section. At low values of Reynolds number and through most of the transition regime, liquid crystal bands oriented in the streamwise direction were visible (Fig. 13). As the Reynolds number increased turbulent forces began to dominate in the curved section, and less evidence could be detected for the existence of the vortices (Fig. 14). Over the entire range of Reynolds numbers studied for the straight section, the liquid crystals formed essentially straight bands perpendicular to the flow direction, indicating approximately two-dimensional flow (Fig. 15). Disruption of flow in the transition region due to the insertion of the sandpaper is illustrated in Figures 16 and 17.

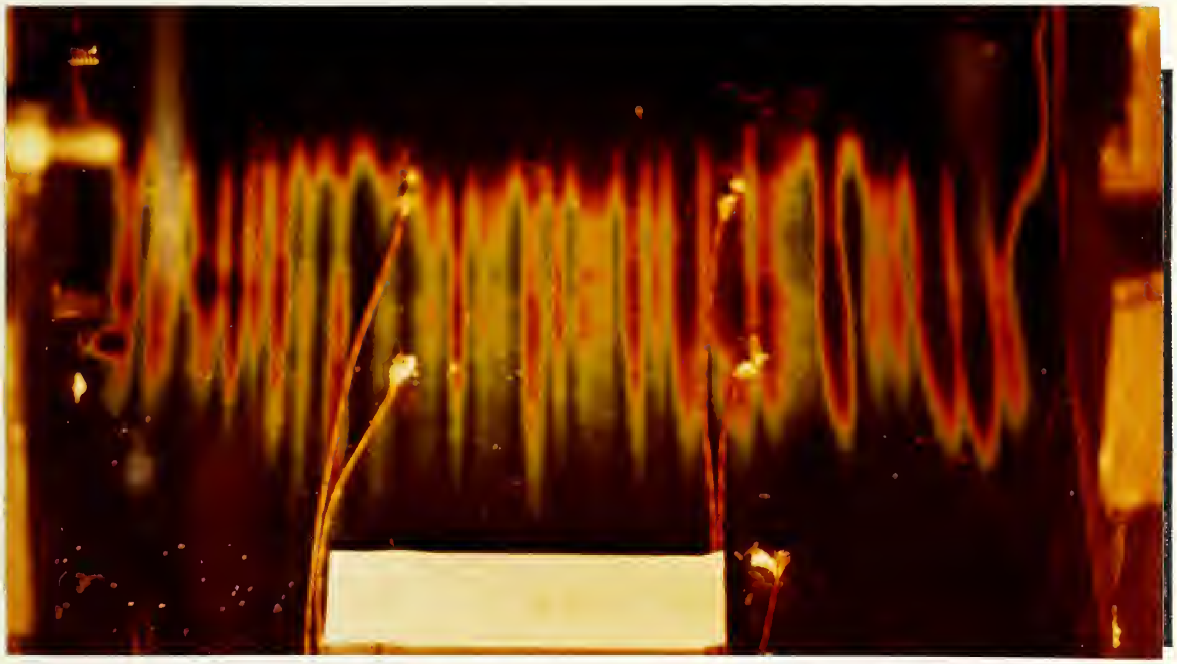

Figure 13. Liquid Crystal Representation of Airflow. (Curved Section, $Re_{hd} = 1100$)

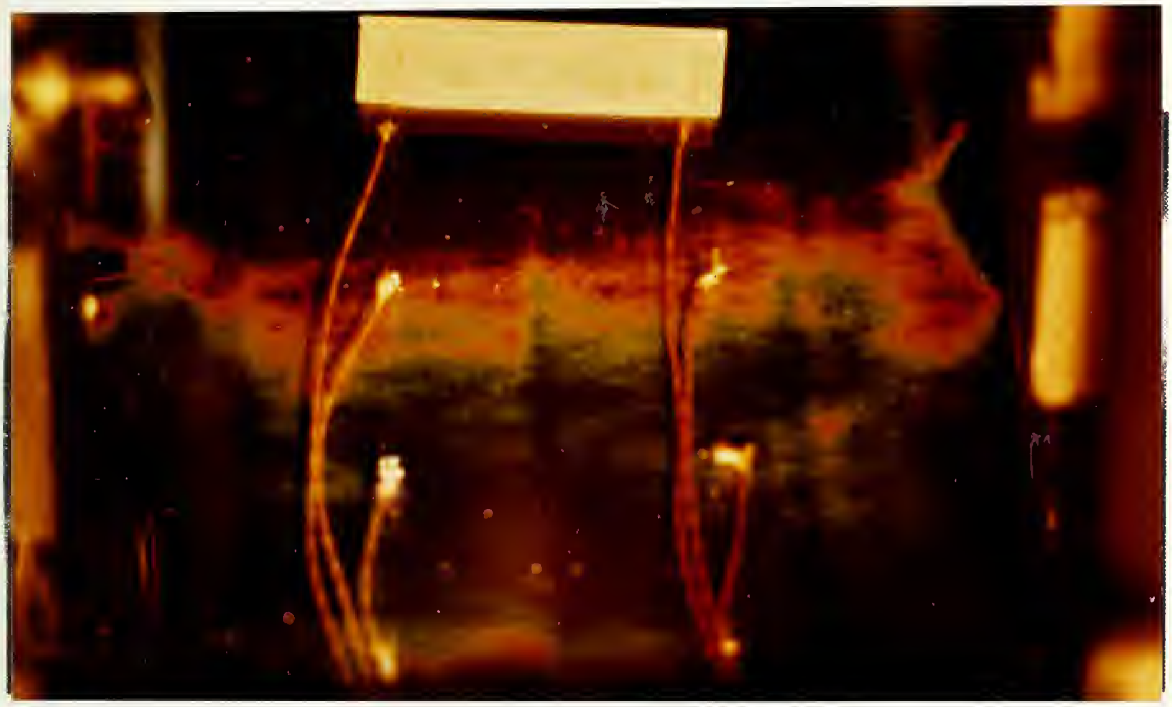

Figure 14. Liquid Crystal Representation of Airflow. (Curved Section, $Re_{hd} = 9400$)

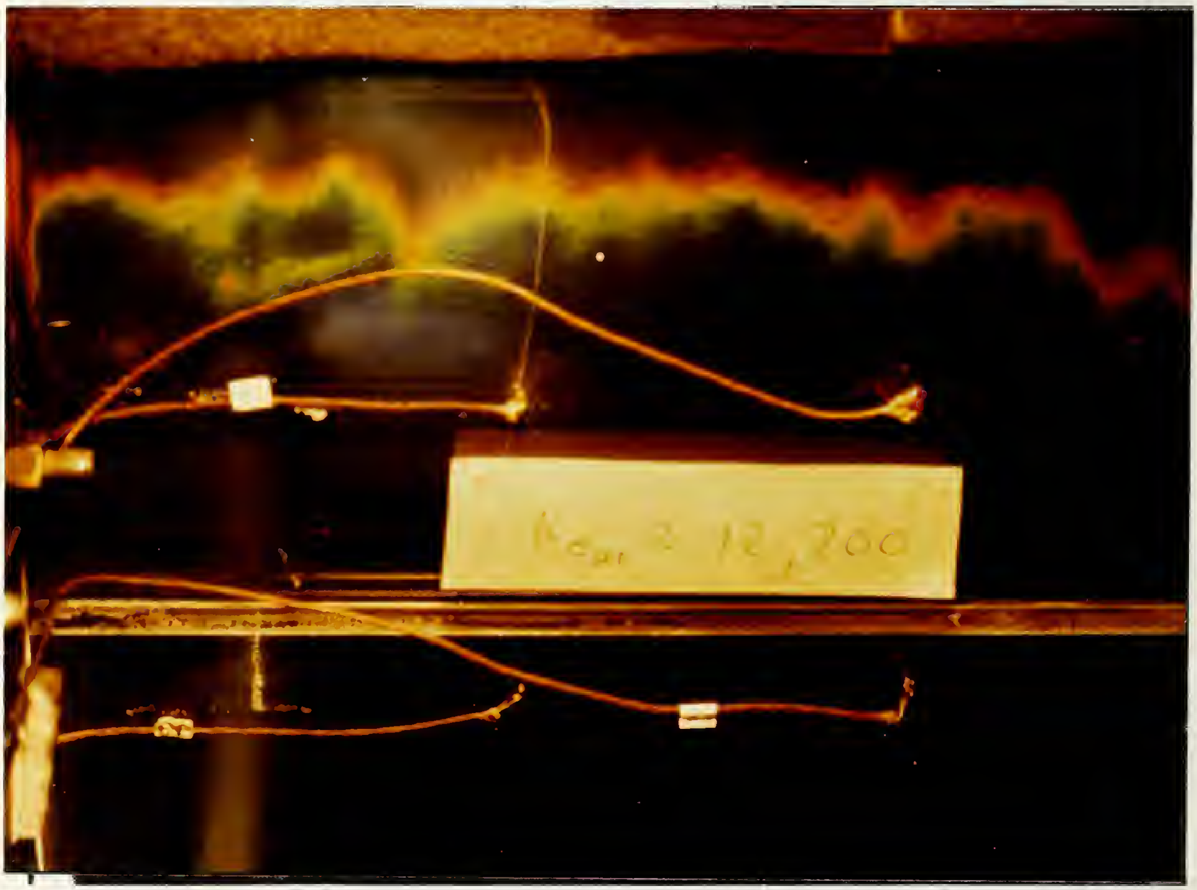

Figure 15. Liquid Crystal Representation of Airflow. (Straight Section, Re_{hd} = 12700)

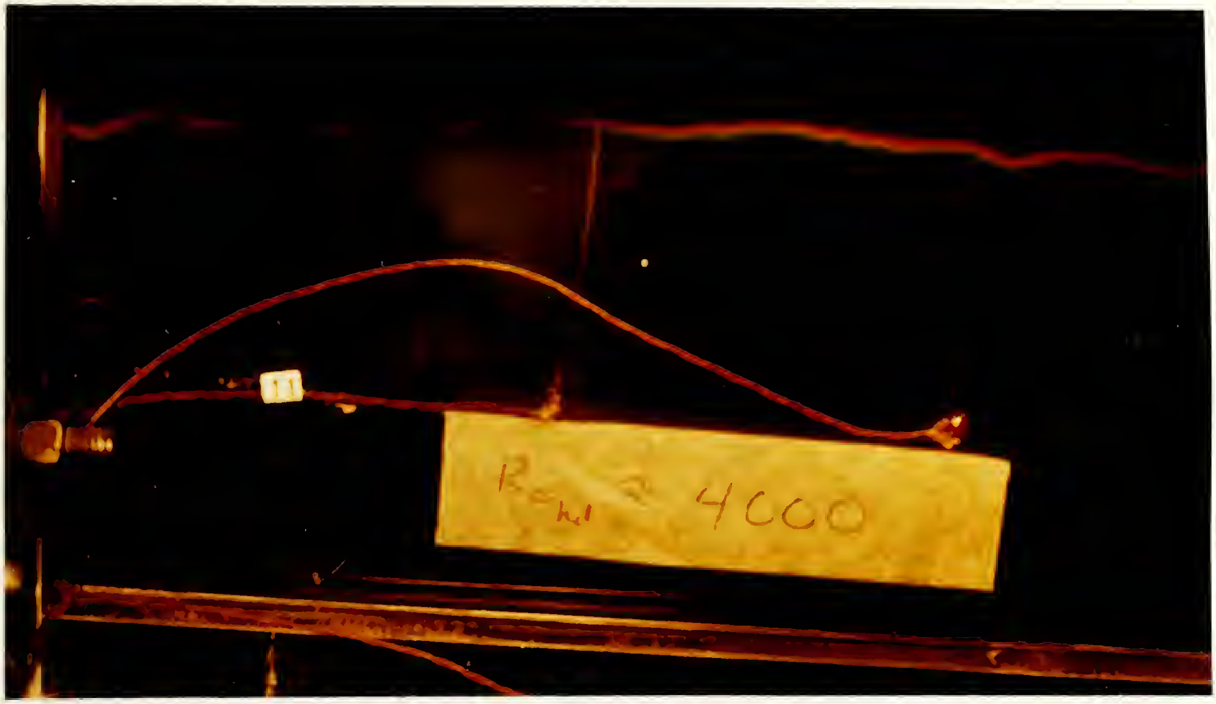

Figure 16. Liquid Crystal Representation of Airflow. (Straight Section, Re_{hd} = 4000, Untripped)

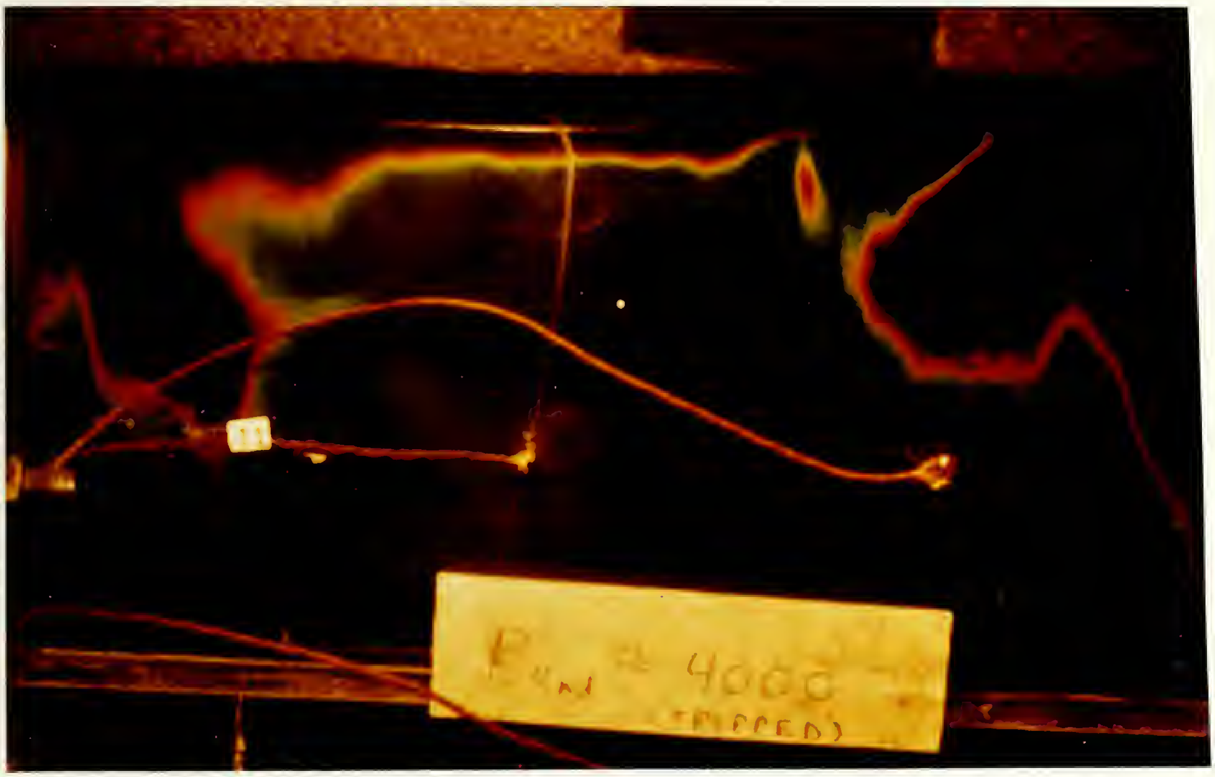
Re_hd ≈ 4000
(TRIPPED)

Figure 17. Liquid Crystal Representation of Airflow. (Straight Section, Re_{hd} = 4000, Tripped)

V. DISCUSSION AND CONCLUSIONS

Holihan [Ref. 24], in his study, determined that there was a negligible difference in the fluid bulk temperature and the unheated wall temperature. He additionally demonstrated that the radiated heat transfer from the unheated wall surface was minimal. These results were verified by Daughety [Ref. 25] for the present study and provide the basis for the assumption that the heat transfer to the air flowing through the channel was solely by convection from the heated Temsheet.

As was mentioned earlier, the high aspect ratio of the channel provided the basis for the assumption that the experimental apparatus, as configured, could be modeled as infinite parallel plates. Holihan's data [Ref. 24] also tended to verify this assumption. His experimental data, in the laminar flow region, approached the theoretical limit for average Nusselt number for parallel plates with one wall heated at a constant heat flux and the opposite wall adiabatic [Ref. 29].

Based on the assumptions mentioned above, comparisons were made with other analytical and experimental results that were of the same or similar problem. Again the problem being, flow between infinite parallel plates with one wall at a constant heat flux and the opposite wall adiabatic.

A comparison of the experimental results of this study and the experimental results of Ballard [Ref. 23], Holihan [Ref. 24] and Daughety [Ref. 25] are shown in Figure 18, for the straight section, and Figure 19 for the curved section. Figure 20 shows a compilation of all the data on one plot. Ballard's data was strictly in the laminar region; Holihan's data covered the laminar as well as transition regions, and Daughety's data was strictly in the turbulent region. The channel aspect ratio was 40 for each of these studies and the experimental procedures were similar in each case. Ballard and Holihan compared their data to the analytical studies by McCuen, [Ref. 30], for heat transfer between infinite parallel plates with constant wall temperatures and heat flux. Daughety compared his data with the results of Shibani and Ozisik [Ref. 19], and Kays and Leung [Ref. 21]. Ballard's and Holihan's data plotted above analytical solutions while Daughety's data plotted below. Differences were attributed to the variations in the geometries used in the studies, side wall effects, inability to account for all of the heat transfer processes, and the limitation inherent in any experimental work.

A comparison of analytical and experimental results with those of the present study for the straight test section is shown graphically in Figure 21. The results of Petuhkov and Popov [Ref. 27] are shown for turbulent heat transfer in round tubes. The correlation used was

REPRODUCED AT GOVERNMENT EXPENSE

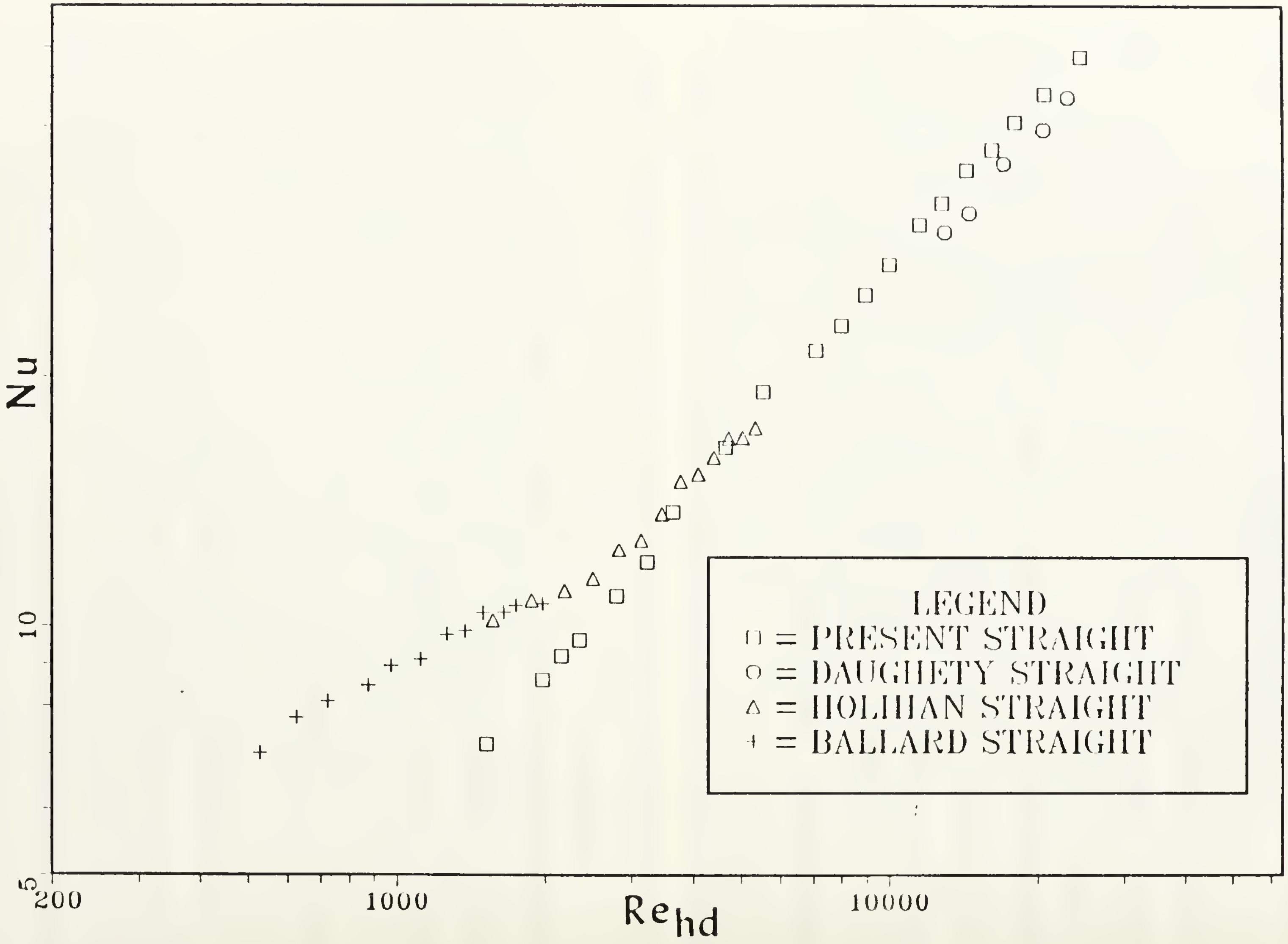

Figure 18. Comparison of Straight Section Present Data with Daughety, Holihan, and Ballard.

REPRODUCED AT GOVERNMENT EXPENSE

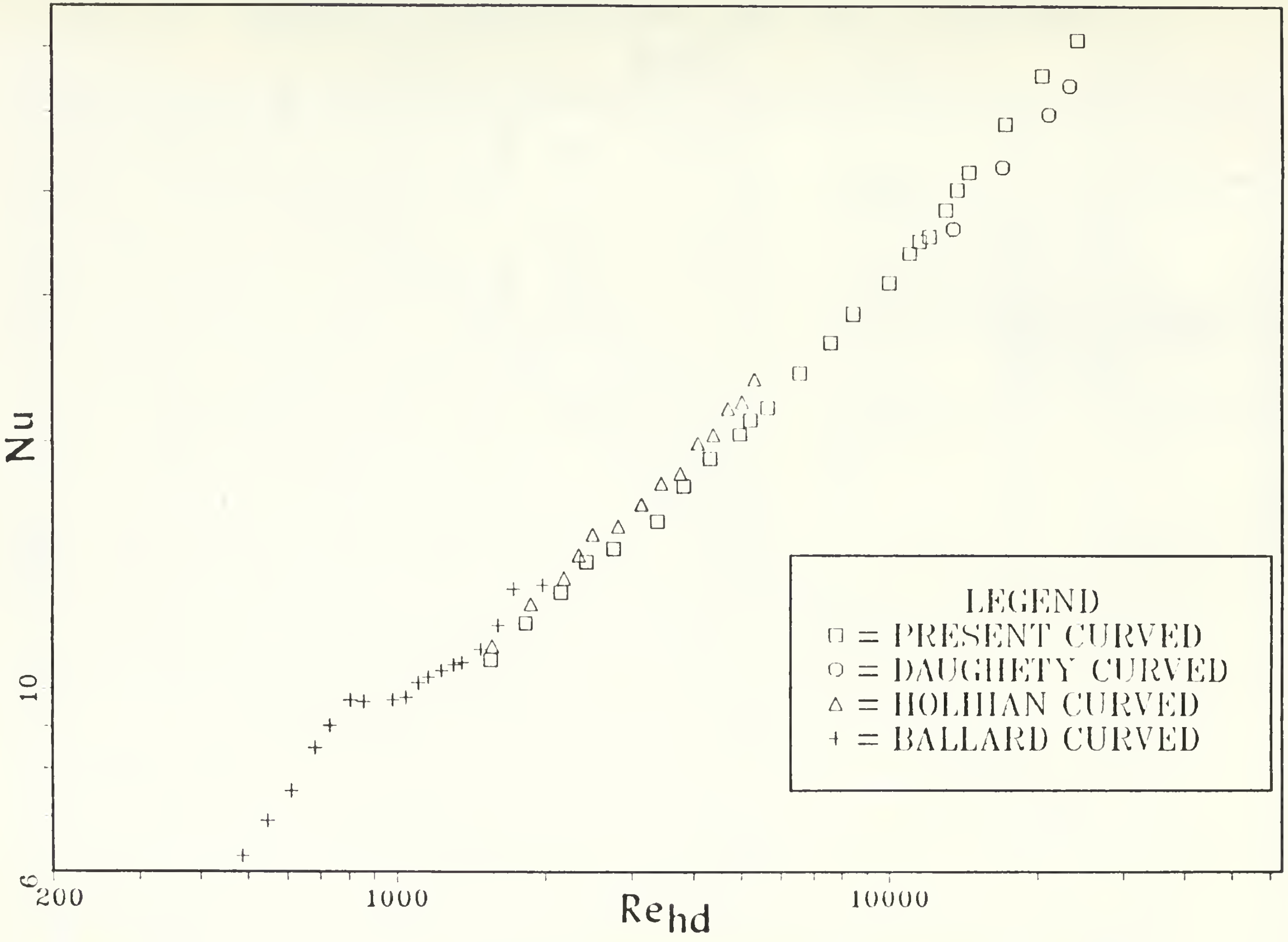

Figure 19. Comparison of Curved Section Present Data with Daughety, Holihan, and Ballard.

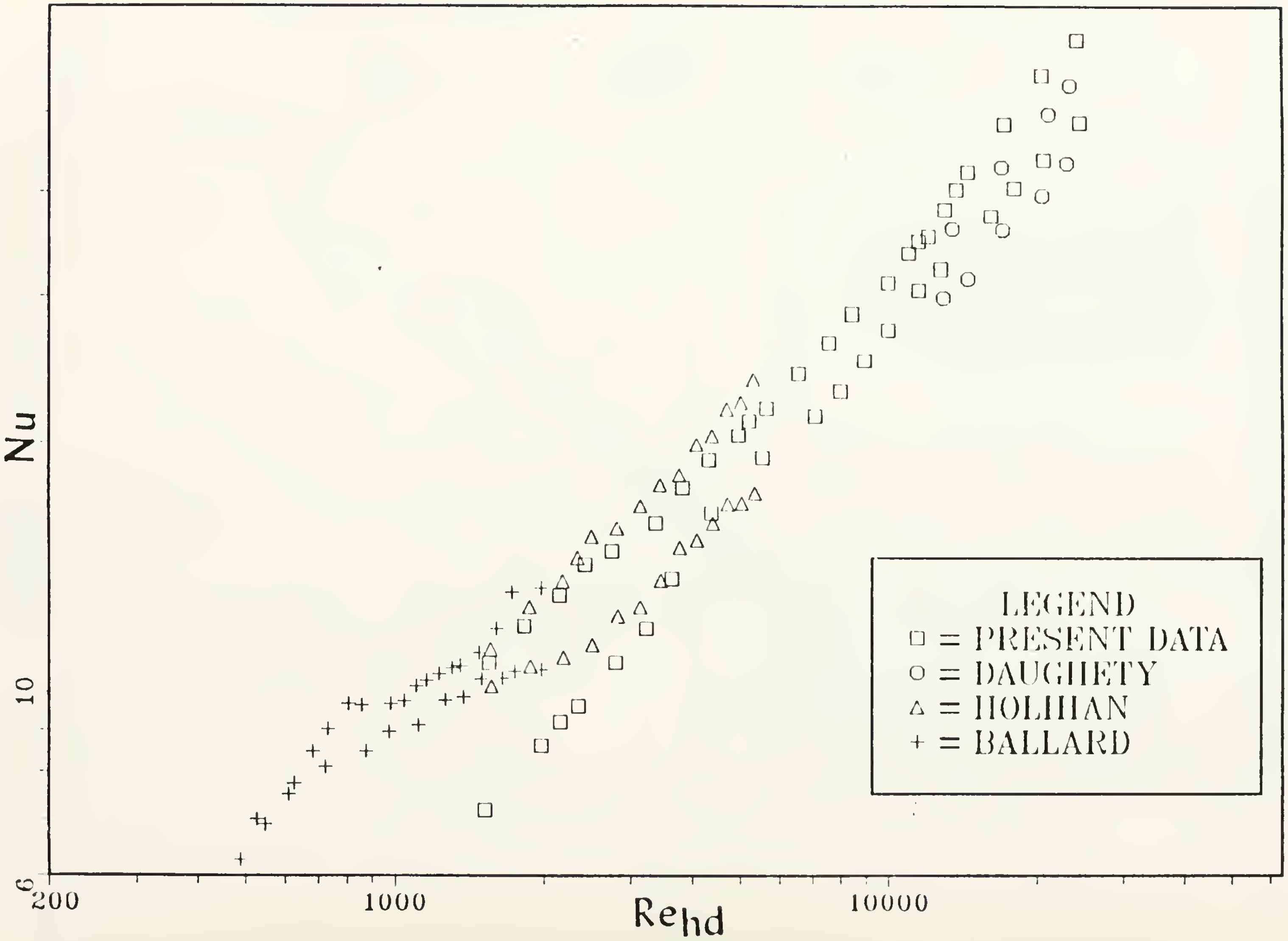

Figure 20. Comparison of Both Sections Present Data with Daughety, Holihan, and Ballard.

REPRODUCED AT GOVERNMENT EXPENSE

$$Nu = \frac{(f/8)\ Re\ Pr}{k_1(f)+k_2(Pr)\sqrt{f/8}(Pr^{(2/3)}-1)}$$

where 'f' the friction factor, has been calculated using the Filonenko equation given in Karlekar and Desmond [Ref. 32] as:

$$f = (1.82 \log Re = 1.64)^{-2}$$

and

$$k_1(f) = 1 + 1.4\ f$$

$$k_2(Pr) = 11.7 + \frac{1.8}{Pr^{(1/3)}}$$

The Dittus-Boelter equation [Ref. 26] for heat transfer in a straight tube for constant wall temperature is plotted from:

$$Nu = 0.02\ Re^{0.08}$$

For a Prandtl number equal to 0.71. Additionally, the results of Kays and Leung [Ref. 21] for heat transfer in annular passages are shown for r* = 1.0, which equates to parallel plates. When extrapolated down these results continue to correlate well with present data.

The curved section data is plotted in Figure 22, and is compared to the experimental work of Brinich and Graham [Ref. 28]. Also plotted as a reference are the analytical solutions of Petukhov and Popov [Ref. 27]. The accuracy of the data points used from Brinich and Graham are subject to

REPRODUCED AT GOVERNMENT EXPENSE

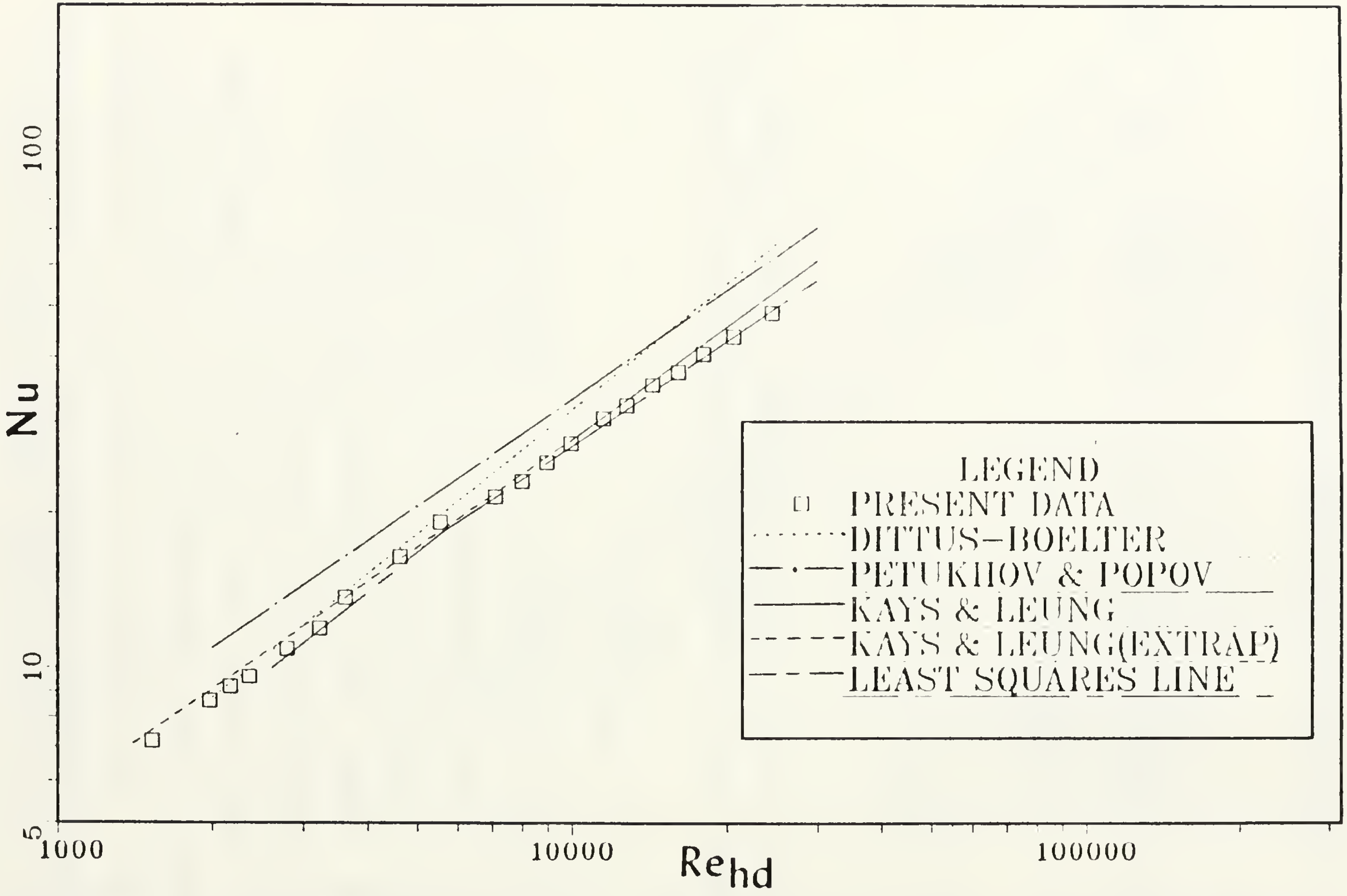

Figure 21. Comparison of Straight Section Present Data with Dittus-Boelter, Petukhov and Popov, Kays and Leung, an Extrapolated Kays and Leung, and a Calculated Least Squares Fit.

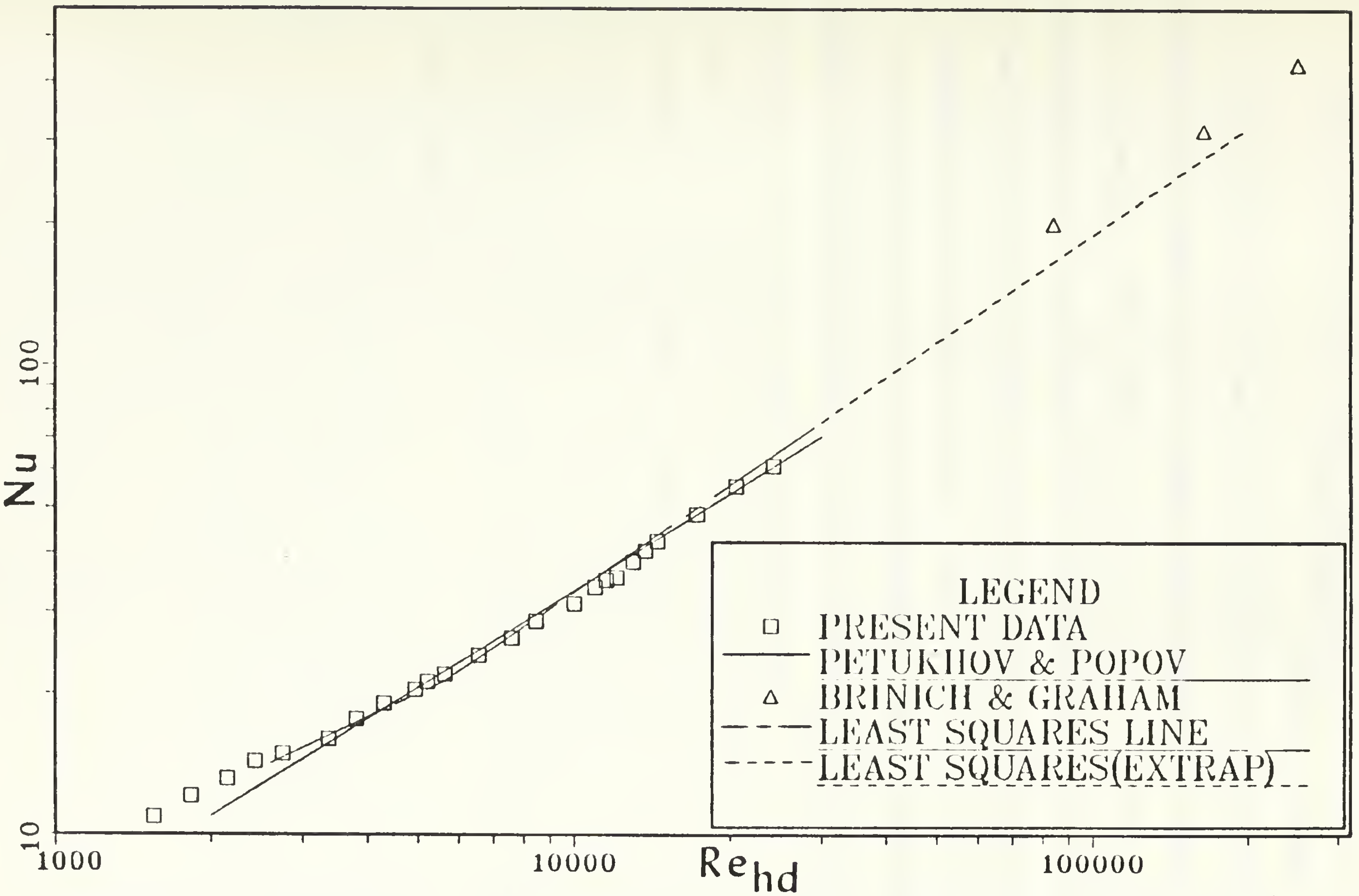

Figure 22. Comparison of Curved Section Present Data with Petukhov and Popov, Brinich and Graham, a Calculated Least Squares Fit, and an Extrapolated Least Squares Fit.

errors, in that the actual values are not given in their study and had to be taken from a plot of Stanton number versus Reynolds number.

Disregarding the small differences between the results and correlations, the trend appears consistent. Heat transfer rates can be seen to increase both with increasing Reynolds number and curvature of the channel. The presence of Taylor-Gortler vortices in the laminar and transition regime seems to be the major contributing factor; whereas increased turbulence, possibly caused by the formation of these vortices, seems to dominate at higher Reynolds numbers.

VI. RECOMMENDATIONS

The amount of experimental work remaining in the study of heat transfer in curved channels is significant. The present experimental apparatus has been used over a range of Reynolds numbers throughout the laminar, transition and into the turbulent regime. Additional experiments probing further into the turbulent regime should be conducted to better understand the heat transfer processes occurring there. This would require a more powerful compressor to generate the higher Reynolds numbers and a larger power supply to sufficiently drive the heated surfaces. Finally, increasing the number of thermocouples at least two-fold and the introduction of pressure transducers which could be connected directly to the data acquisition system would both prove to increase the accuracy and reliability of the experimental apparatus.

To gain further insight into the effect of curvature on the rate of heat transfer, additional boundary conditions for the test should also be considered. An apparatus possessing a heated wall on each side of the test section might be one such consideration.

APPENDIX A: EXPERIMENTAL UNCERTAINTY

The uncertainties for the major variable in the experiments, were calculated in accordance with the method described by S. Kline and F. McClintoch [Ref. 29]. The estimates of the uncertainty in the measured quantities were made conservatively. As a result, there is considerable confidence in the uncertainties as calculated.

The following equations were used to calculate the uncertainties:

$$(1)\ d\dot{m} = \dot{m}\ [((\frac{dY}{Y})^2 + (\frac{dK}{K})^2 + (\frac{dA}{A})^2) + (1/4\ ((\frac{d\rho_{air}}{\rho_{air}})^2 + (\frac{d\Delta P}{\Delta P})^2))]^{1/2}$$

$$(2)\ dQ_{air} = Q_{air}\ ((\frac{d\dot{m}}{\dot{m}})^2 + (\frac{d\ C_{pair}}{C_{pair}})^2 + (\frac{d(T_{out}-T_{in})}{T_{out}-T_{in}})^2)^{1/2}$$

$$(3)\ d\overline{h} = \overline{h}\ ((\frac{dQ_{air}}{Q_{air}})^2 + (\frac{dA_{PL}}{A_{PL}})^2 + (\frac{d\Delta T}{\Delta T})^2)^{1/2}$$

$$(4)\ d\overline{Nu} = \overline{Nu}\ ((\frac{d\overline{h}}{\overline{h}})^2 + (\frac{dD_{hd}}{D_{hd}})^2 + (\frac{dK_{air}}{K_{air}})^2)^{1/2}$$

$$(5)\ dRe_{hd} = Re_{hd}\ ((\frac{d\dot{m}}{\dot{m}})^2 + (\frac{dD_{hd}}{D_{hd}})^2 + (\frac{d\mu_{air}}{\mu_{air}})^2 + (\frac{dA_c}{A_c})^2)^{1/2}$$

The values obtained for the uncertainties for the values in the curved section test run at a Reynolds number of 13000 are:

Quantity	Uncertainty
A	.0348
A_{PL}	.0019
A_c	.0438
C_p	.0020
D_{hd}	.0236
$\overline{h}$	.0058
K	.0008
K_{air}	.0038
$\overline{Nu}$	.0127
$\dot{m}$	.0050
Q_{air}	.0058
Re_{hd}	.0289
T_{blk}	.0004
T_{in}	.0004
T_{out}	.0004
T_{wo}	.0002
$T_{out}-T_{in}$	.0027
Y	.0024
ΔP	.0500
ΔT	.0005
μ_{air}	.0054
ρ_{air}	.0001

The major source of uncertainty in the average Nusselt number is the uncertainty in the pressure readings from the manometer, which affects the mass flow rate calculation. In order to obtain a more accurate pressure measurement, it has been recommended that pressure transducers be used instead of vertical manometers in future studies.

APPENDIX B: SAMPLE CALCULATIONS

Figure 23 below, shows the major heat transfer components for each of the test sections. The sample calculations that follow, demonstrate the methods used by the computer to calculate these components as well as the Reynold's number, average heat transfer coefficient, and average Nusselt number for each set of data. The sample calculations are for the curved section, but those for the straight section are similar. Reynolds number, Nusselt number, and Dean number are based on hydraulic diameter.

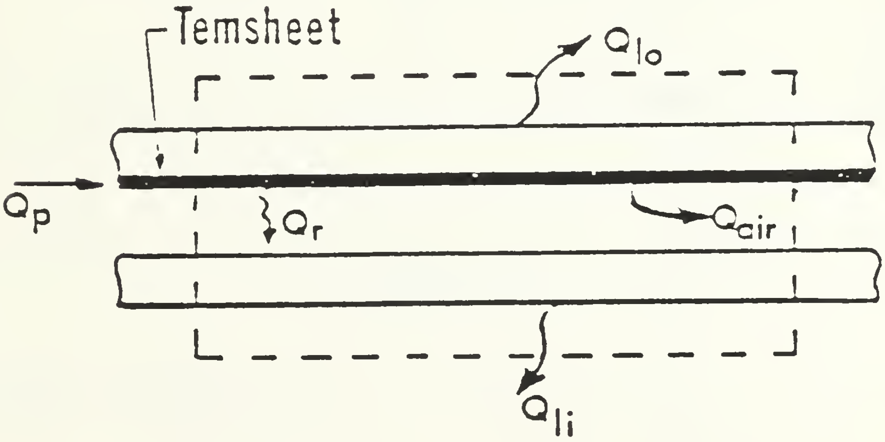

Figure 23. Energy Balance in Straight Section.

A. SAMPLE CALCULATION DATA

V_H = 55.28 V

V_R = 4.53 V

R_{PR} = 2.0262 Ω

P_{atm} = 30.11 in. Hg

ΔP = 12.00 in. H_2O

P_1 = 8.50 in. H_2O

T_{in} = 23.01 C

T_{out} = 26.78 C

T_{wo} = 44.74 C

T_{wi} = 24.64 C

T_{ins1} = 39.67 C

T_{ins2} = 33.38 C

T_{orif} = 26.57 C

K_{air} = 26.22×10^{-3} W/mK

C_{pair} = 1006 J/Kg K

μ_{air} = 18.59×10^{-6} Kg/ms

K_{ins} = 3.6495×10^{-2} W/mK

ΔX_{ins} = 0.01270 m

ε_{wo} = 0.70

ε_{wi} = 0.40

σ = 5.669×10^{-8} W/m^2K^4

β = .5325

γ = 1.402

gc = 1 Kg m/NS^2

R = 286.8 Nm/Kg K

$F_{wo-wi} = 1.0$

$A_{PL} = .0730\ m^2$

$A_c = .0016\ m^2$

$A_{pipe} = .002027\ m^2$

$D_c = .00635\ m$

$D_{pipe} = .0508\ m$

$D_{orif} = .027051\ m$

$P_{wet} = .5207\ m$

B. TEMPERATURE CALCULATIONS

1. Bulk Temperature (T_{blk})

$$T_{blk} = \frac{T_{in} + T_{out}}{2} = \frac{23.01 + 26.78}{2} = 24.90\ C$$

2. Mean Temperature Difference (ΔT)

$$\Delta T = T_{wo} - T_{blk} = 44.74 - 24.90 = 19.85\ C$$

3. Temperature Difference in the Insulation (ΔT_{ins})

$$\Delta T_{ins} = T_{ins1} - T_{ins2} = 39.67 - 33.38 = 6.29\ C$$

C. POWER CALCULATIONS

1. Power Supplied (Q_p)

$$Q_p = \frac{V_H \; V_R}{R_{PR}} = \frac{(55.28)\;(4.53)}{(2.0262)} = 123.59 \text{ W}$$

2. Heat Lost Through the Outer Plate (Q_{lo})

$$Q_{lo} = \frac{\Delta T_{ins}}{(\Delta X_{ins})/(K_{ins})(A_{PL})} = \frac{6.29}{(0.0127)/(3.6495\text{x}10^{-2})(.0730)}$$

$$= 1.32 \text{ W}$$

3. Heat Radiated (Q_r)

a. Radiation Resistance (R_R)

$$R_R = \frac{1 - \varepsilon_{wo}}{A_{PL}\,\varepsilon_{wo}} + \frac{1}{A_{PL}\;F_{wo-wi}} + \frac{1 - \varepsilon_{wi}}{A_{PL}\,\varepsilon_{wi}}$$

$$= \frac{1}{A_{PL}}\left[\frac{1}{\varepsilon_{wo}} + \frac{1}{\varepsilon_{wi}} - 1\right] = \frac{1}{(0.0730)}\left[\frac{1}{0.7}+\frac{1}{0.4}-1\right]=40.12 \text{ m}^{-2}$$

b. Heat Radiated (Q_r)

$$Q_r = \frac{\sigma(T_{wo}^{\;2} - T_{wi}^{\;4})}{R_R} \qquad T[=]K$$

$$= \frac{(5.669\text{x}10^{-8})[(44.74+273)^4 - (24.64+273)^4]}{40.12}$$

$$= 3.31 \text{ W}$$

D. MASS FLOW RATE CALCULATIONS

1. Pressure Conversions

a. P_{atm}=30.11 in. Hg x 3374.1 = 101594.15 N/m^2

b. $\Delta P = 12.0 \text{ in. } H_2O \times 248.64 = 2983.68 \text{ N/m}^2$

c. $P_1 = (8.5 \text{ in. } H_2O \times 248.64) + 101594.15 = 103707.59 \text{ N/m}^2$

2. Density of Air (ρ_{air})

$$\rho_{air} = \frac{P_{atm}}{R\, T_{orif}} = \frac{(101594.15)}{(286.8)(26.57+273)} = 1.1825 \text{ Kg/m}^3$$

3. Expansion Factor (Y)

$$Y = 1-[0.333+1.145(\beta^2+0.7\beta^5+12\beta^{13})]\ \frac{\Delta P}{\gamma P_1}$$

$$= 1-[0.333+1.145((.5325)^2+0.7(.5325)^5+12(.5325)^{13})] \times \frac{2983.68}{(1.402)(103707.59)}$$

$$= .9857$$

4. Area of Orifice (A)

$$A = \frac{\pi(D_{orif})^2}{4} = \frac{\pi(.02705)^2}{4} = .0005747 \text{ m}^2$$

5. Mass Flow Rate ($\dot{m}$)

$$\dot{m} = YKA\sqrt{2gc\rho_{air}\ \Delta P} = (.9857)K(.0005747) \times \sqrt{2(1)(1.1825)(2983.68)}$$

$$\dot{m} = .04759\ K$$

Iterating:

Assume a Reynolds number $_{pipe}$ = 40000

Obtain a value for K, the flow coefficient, from reference 30. K = .6350

Solve for $\dot{m}$. $\dot{m} = .0302$ Kg/s

Solve for new $Re_{pipe} = \frac{m\ D_{pipe}}{A_{pipe}\mu_{air}} = \frac{(.0302)\ (.0508)}{(.002027)(18.59\text{x}10^{-6})}$

$Re_{pipe} = 40713$

Check convergence and repeat process if necessary.

(Convergence if difference less than .001)

$\dot{m} = .0302$ Kg/s

E. REYNOLDS NUMBER CALCULATIONS

1. $Re_{pipe} = \frac{\dot{m}\ D_{pipe}}{A_{pipe}\mu_{air}} = \frac{(.0302)\ \ (.0508)}{(.002027)(18.59\text{x}10^{-6}} = 40713$

2. $Re_{d} = \frac{\dot{m}\ D_{c}}{A_{c}\ \mu_{air}} = \frac{(.0302)\ \ (.00635)}{(.0016)(18.59\text{x}10^{-6}} = 6447$

3. $Re_{hd} = \frac{\dot{m}\ D_{hd}}{A_{c}\ \mu_{air}}$

   a. $D_{hd} = \frac{4 \text{ x } A_{c}}{P_{wet}} = \frac{(4)\ (.0016)}{.5207} = .01229$ m

   $Re_{hd} = \frac{\dot{m}\ D_{hd}}{A_{c}\ \mu_{air}} = \frac{(.0302)\ (.01229)}{(.0016)(18.59\text{x}10^{-6}} = 12478$

F. HEAT CONVECTED TO AIR CALCULATION

1. $Q_{air} = \dot{m}C_{p}(T_{out}-T_{in}) = (.0302)(1006)(26.78-23.01)=114.54$ W

G. AVERAGE HEAT TRANSFER COEFFICIENT CALCULATION

$$\bar{h} = \frac{Q_{air}}{A_{PL}\ \Delta T} = \frac{114.54}{(.0730)(19.84)} = 79.08\ \mathrm{W/m^2C}$$

H. AVERAGE NUSSELT NUMBER CALCULATION

$$\overline{Nu} = \frac{\bar{h}\ D_{hd}}{K_{air}} = \frac{(79.08)\ (.01229)}{26.22 \times 10^{-3}} = 37.07$$

I. DEAN NUMBER CALCULATION

$$De = Re_p \sqrt{\frac{Dc}{Ri}} = 40713 \sqrt{\frac{.00635}{.305}} = 5875$$

APPENDIX C: CORRELATIONS

The correlations obtained for the present study were obtained using the method of least squares for a first degree polynomial, as outlined by C. F. Gerald [Ref. 31]. In this method the values of Reynolds number (x) and Nusselt number (Y) were first converted to their natural logarithmic value. Next the summations of x_i, x_i^2, Y_i, and x_iY_i were calculated. The values of these quantities were then placed in a matrix:

$$\begin{bmatrix} N & \Sigma x_i \\ \Sigma x_i & \Sigma x_i^2 \end{bmatrix} \begin{bmatrix} a_o \\ a_1 \end{bmatrix} = \begin{bmatrix} \Sigma Y_i \\ \Sigma x_i Y_i \end{bmatrix}$$

and the resulting simultaneous equations

$$a_oN + a_1\Sigma x_i = \Sigma Y_i$$

$$a_o\Sigma x_i + a_1\Sigma x_i^2 = \Sigma x_iY_i$$

were solved for a_o and a_1.

The equation of the line then became:

$$\text{Ln } \overline{Nu} = a_o + a_1 \text{Ln Re}$$

or

$$\overline{Nu} = e^{a_o} \quad Re^{a_1}$$

The standard error for the present study correlation was calculated by the following equation:

$$\sigma^2 = \frac{\Sigma(Y_i - Y_i)}{N - n - 1}$$

where: Y_i is the actual value of the average Nusselt number obtained experimentally.

y_i is the value of the average Nusselt number calculated from the correlation equation.

N is the number of data points used in the correlation.

n is the degree of the polynomial used.

LIST OF REFERENCES

1. Taylor, G. I., "Stability of a Viscous Liquid Contained Between Two Rotating Cylinders," Philosophical Transactions of the Royal Society of London, series A, V.233, pp. 289-343, 1923.

2. National Advisory Committee for Aeronautics, Technical Memorandum 1375, On the Three Dimensional Instability of Laminar Boundary Layers on Concave Walls, by H. Gortler, 1942.

3. Smith, A.M.O., "On the Growth of Taylor-Gortler Vortices Along Highly Concave Walls," Quarterly of Applied Mathematics, V. 8, pp. 233-263, November 1955.

4. Dement'eva, K. V. and Aronov, I. Z.,"Hydrodynamics and Heat Transfer in Curvelinear Channels of Rectangular Cross Section," Journal of Engineering Physics, V. 34, No. 6, pp. 666-671, 1978.

5. Mayle, R. E., Kopper, F. C., Blair, M. F., and Bailey, D. A., "Effect of Streamline Curvature on Film Cooling," Journal of Engineering for Power, Trans. ASME, V. 99, Series A, No. 1, pp. 77-82, January 1977.

6. Nicolas, J. and LeMeur, A., "Curvature Effects on a Turbine Blade Cooling Film," ASME Paper No. 74-GT-156, 1974.

7. Folayan, C. O. and Whitelaw, J. H., "The Effectiveness of Two-Dimensional Film-Cooling Over Curved Surfaces," ASME Paper No. 76-HT-31, 1976.

8. Lord Raleigh, "On the Dynamics of Revolving Fluids," Proceedings of the Royal Society of London, Series A, V. 93, pp. 148-154, 1916. Reprints in Scientific Papers, V. 6, pp. 447-453.

9. Taylor, G. I., "Distribution of Velocity and Temperature Between Concentric Rotating Cylinders," Proceedings of the Royal Society of London, Series A, V. 151, pp. 494-512, 1935.

10. Dean, W. R., "Fluid Motion in a Curved Channel," Proceedings of the Royal Society of London, Series A, V. 121, pp. 402-420, 1928.

11. Reid, W. H., "On the Stability of Viscous Flow in a Curved Channel," Proceedings of the Royal Society of London, Series A, V. 244, pp. 186-198, 1958.

12. Schlichting, H., Boundary Layer Theory, 7th Ed., pp. 529-536, McGraw-Hill, 1979.

13. Kelleher, M. D., Flentie, D. L., and McKee, R. J., "An Experimental Study of the Secondary Flow in a Curved Rectangular Channel," Journal of Fluids Engineering, V. 102, pp. 92-96, March 1980.

14. Winoto, S. H., Durao, D.F.G., and Crane, R. I., "Measurement within Gortler Vortices," Journal of Fluids Engineering, V. 101, pp. 517-520, December 1979.

15. Aihara, Y., "Nonlinear Analysis of Gortler Vortices," The Physics of Fluids, V. 19, pp. 1655-1660, November 1976.

16. Kreith, F., "The Influence of Curvature on Heat Transfer to Incompressible Fluids," Trans. ASME, V. 77, pp. 1247-1256, 1955.

17. Aerospace Research Laboratories Report ARL 65-68, A Simplified Approach to the Influence of Gortler-Type Vortices on the Heat-Transfer from a Wall, by Leif N. Persen, May 1965.

18. Cheng, K. C., and Akiyama, M., "Laminar Forced Convection Heat Transfer in Curved Rectangular Channels," International Journal of Heat and Mass Transfer, V. 13, pp. 471-490, 1970.

19. Shibani, A. A., and Ozisik, M. N., "A Solution to Heat Transfer in Turbulent Flow Between Parallel Plates," International Journal of Heat and Mass Transfer, V. 20, pp. 65-573, 1977.

20. Mori, Y., Uchida, Y., and Ukon, T., "Forced Convective Heat Transfer in a Curved Channel with a Square Cross Section," International Journal of Heat and Mass Transfer, V. 14, pp. 1787-1805, 1971.

21. Kays, W. M. and Leung, E. Y., "Heat Transfer in Annular Passages - Hydrodynamically Developed Turbulent Flow with Arbitrarily Prescribed Heat Flux," International Journal of Heat and Mass Transfer, V. 6, pp. 507-557, 1963.

22. Durao, M. do Carmo, Investigation of Heat Transfer in Straight and Curved Rectangular Ducts Using Liquid Crystal Thermography, M.S. Thesis, Naval Postgraduate School, Monterey, California, 1977.

23. Ballard, J. C. III, Investigation of Heat Transfer in Straight and Curved Rectangular Ducts, M.S. Thesis, Naval Postgraduate School, Monterey, California, 1980.

24. Holihan, R. G., Jr., Investigation of Heat Transfer in Straight and Curved Rectangular Ducts for Laminar and Transition Flows, M.S. Thesis, Naval Postgraduate School, Monterey, California, 1980.

25. Daughety, S. F., Experimental Investigation of Turbulent Heat Transfer in Straight and Curved Rectangular Ducts, M.S. Thesis, Naval Postgraduate School, Monterey, California, 1983.

26. Gebhart, B., Heat Transfer, 2nd Ed., p. 260, McGraw-Hill, New York, 1971.

27. Petukhov, B. S. and Popov, V. N., "Theoretical Calculation of Heat Exchange and Frictional Resistance in Turbulent Flow in Tubes of an Incompressible Fluid with Variable Physical Properties," Trans. in High Temperatures, V. 1, No. 1, pp. 69-83, 1963.

28. Brinich, P. F. and Graham, R. W., Flow and Heat Transfer in a Curved Channel, NASA Technical Note No. TN-D-8464, 1977.

29. Shah, R. K. and London, A. L., Laminar Flow Forced Convection in Ducts, Supplement 1, pp. 305-312, Academic Press, 1978.

30. Department of Mechanical Engineering, Stanford University, Report No. AHT-3, Heat Transfer with Laminar and Turbulent Flow Between Parallel Planes with Constant and Variable Wall Temperature and Heat Flux, by P. A. McCuen, W. M. Kays, and W. C. Reynolds, 12 April 1982.

31. Kline, S. J. and McClintock, F. A., "Describing Uncertainties in Single-Sample Experiments," Mechanical Engineering, V. 75, pp. 3-8, January 1953.

32. Karlekar, B. V. and Desmond, R. M., Engineering Heat Transfer, p. 560, West Publishing Company, 1977.

33. The American Society of Mechanical Engineers, Supplement to ASME Power Test Codes, Chapter 4, Flow Measurement, p. 25, 1959.

INITIAL DISTRIBUTION LIST

		No. Copies
1.	Defense Technical Information Center Cameron Station Alexandria, Virginia 22314	2
2.	Library, Code 0142 Naval Postgraduate School Monterey, California 93943	2
3.	Department Chairman, Code 69 Department of Mechanical Engineering Naval Postgraduate School Monterey, California 93943	1
4.	Professor M. D. Kelleher, Code 69Kk Department of Mechanical Engineering Naval Postgraduate School Monterey, California 93943	2
5.	Lieutenant Joel L. Wilson, USN 104 Blair Mill Road Hatboro, Pennsylvania 19040	2

197-619

213233

Thesis
W6387
c.1

Wilson

Experimental investigation of turbulent heat transfer in straight and curved rectangular ducts.

213233

Thesis
W6387
c.1

Wilson

Experimental investigation of turbulent heat transfer in straight and curved rectangular ducts.

thesW6387
Experimental investigation of turbulent
3 2768 000 61643 7
DUDLEY KNOX LIBRARY